

Supporting information for

Symmetry Breaking Charge Transfer of Visible Light Absorbing System

Cong Trinh,¹ Kent Kirlikovali,¹ Saptaparna Das,¹ Maraia E Ener,² Harry B Gray,² Peter Djurovich,¹ Stephen E Bradforth,¹ Mark E Thompson.^{1*}

¹Department of Chemistry, University of Southern California, Los Angeles, California 90089

²California Institute of Technology, 1200 E California Blvd, Pasadena California 91125

Table of Content

1. Synthesis and Characterization of zDIP1-zDIP4 , zDIP2' and zDIP3'	S3
2. Global Analysis of Femtosecond Transient absorption spectra.....	S6
3. Femtosecond Excited State Dynamics of zDIP2 and zDIP3	S7
4. Comparison between Spectro-electrochemistry and TA measurements of zDIP1	S8
5. Figure S1. ¹ H NMR of zDIP3	S9
6. Figure S2. ¹³ C NMR of zDIP3	S10
7. Figure S3. ¹ H NMR of zDIP4	S11
8. Figure S4. ¹³ C NMR of zDIP4	S12
9. Figure S5. ¹ H NMR of zDIP5 in CDCl ₃ over time.....	S13
10. Figure S6. ¹³ C NMR of zDIP5 in CDCl ₃	S14
11. Figure S7. ¹ H NMR of zDIP6 in CDCl ₃ over time.....	S15
12. Figure S8. ¹³ C NMR of zDIP6 in CDCl ₃	S16
13. Figure S9. Absorption spectra of zDIP1-4 in different solvents	S17
14. Figure S10. Emission spectra of zDIP1 , zDIP3 and zDIP4 in different solvents	S18
15. Figure S11. Emission and absorption intensities of zDIP2 solution in dichloromethane at various concentrations.	S19
16. Figure S12. Emission spectra of zDIP1-4 in 2MeTHF at 77K.....	S20
17. Figure S13. Absorption spectra of zDIP5 and zDIP6 in different solvents.....	S21
18. Figure S14. Emission spectra of zDIP6 in different solvents	S22
19. Figure S15. Emission spectra of zDIP1-4 in 2MeTHF at 77K.....	S23
20. Figure S16. Electrochemistry measurements of zDIP1-4 in THF.....	S24
21. Figure S17. Electron density surfaces of zDIP1 and zDIP2	S25
22. Figure S18. DADS used to fit the transient spectra of zDIP1 in various solvents.....	S26
23. Figure S19. Femtosecond TA of zDIP2 in cyclohexane and toluene.....	S27
24. Figure S20. DADS used to fit the transient spectra of zDIP2 in various solvents.....	S28
25. Figure S21. Femtosecond TA of zDIP3 in cyclohexane, toluene and acetonitrile.....	S29

26. Figure S22. DADS used to fit the transient spectra of zDIP3 in various solvents.....	S30
27. Figure S23. Normalized photoluminescence measurements of zDIP1-3 in different polarity solvents.....	S31
28. Figure S24. Electrochemistry and spectroelectrochemistry measurements of zDIP1 in dichloromethane.....	S32
29. Figure S25. Spectral lineshape comparison between spectro-electrochemistry and TA measurements of zDIP1 in dichloromethane.....	S33
30. Figure S25. Microsecond TA of zDIP1 in cyclohexane and toluene	S34
31. Figure S26. Ortep diagrams of zDIP2 and zDIP5	S35
32. Table S1. Photophysical properties of zDIP1-6 in different solvents.	S36-37
33. X-ray data collection and structural determination of zDIP3	S38-40
34. X-ray data collection and structural determination of zDIP4	S41-43
35. X-ray data collection and structural determination of zDIP5	S44-46
36. X-ray data collection and structural determination of zDIP6	S47-49
37. Fitting parameters for the PL lifetime measurements of zDIP1-3 in different solutions..	S50

Synthesis and Characterization:

Synthesis of homoleptic complexes *zDIP1*–*zDIP4*. 2,4-dimethylpyrrole (98%) and 3-ethyl-2,4-dimethylpyrrole were purchased from TCI America; 2-methylpyrrole was synthesized by published procedure; synthesis of *zDIP1* followed the literature procedures.⁴² The obtained *zDIP1* was further purified by vacuum sublimation. Syntheses of *zDIP2*–*zDIP4* were modified from the literature procedures for *zDIP1*. The synthetic procedure for preparing *zDIP2* is given below; the same procedure was used to prepare *zDIP3* and *zDIP4*.

Bis(1,9-dimethyl-5-mesityldipyrinato) zinc (zDIP2). A solution of mesitaldehyde (4.6 g, 30.9 mmol) and 2-methylpyrrole (5 g, 61.7 mmol) in 200 ml dichloromethane was prepared and 3 drops of trifluoroacetic acid (TFA) were added to the rapidly stirred solution under nitrogen. After stirring for 6 hours, the reaction was quenched with 3 ml of triethylamine. The reaction mixture was washed with a saturated solution of Na₂CO₃ in water (100 ml, 3 times), and brine (100 ml, 1 time), and dried over anhydrous Na₂SO₄. The solvent was then removed under reduced pressure to obtain the viscous pale yellow liquid which solidifies upon standing at room temperature; the yield was quantitative. The product 1,9-dimethyl-5-mesityldipyrromethane was used without further purification.

A solution of 1,9-dimethyl-5-mesityldipyrromethane in 250 ml freshly distilled tetrahydrofuran (THF) was prepared, and a solution of 2,3-dichloro-5,6-dicyano-1,4-benzoquinone (DDQ) (7.02 g, 30.9 mmol) in 35 ml of THF was added slowly to the stirred solution under nitrogen. After stirring for 1 hour, the reaction was quenched with 10 ml of triethylamine. The solvent was removed under reduced pressure. The product mixture was dissolved in 500 ml of dichloromethane, and the solution was washed with saturated NaHCO₃ solution (250 ml, 3 times) and brine (250 ml, 1 time). The solution was then dried over anhydrous Na₂SO₄ and filtered. The product 1,9-dimethyl-5-mesityldipyrromethene was used for the next step without further purification.

A solution of zinc acetate dihydrate (Zn(OAc)₂•2H₂O) (20 g, 91 mmol) in 100 ml of methanol was added to the solution of 1,9-dimethyl-5-mesityldipyrromethene in dichloromethane under air. The reaction mixture was stirred overnight. After that, the reaction mixture was filtered using filter paper, and the

solvents were removed under reduced pressure yielding a dark red solid. The obtained solid was passed through a short neutral alumina plug using hexanes/dichloromethane (7/3) mixture as eluent; the orange-red portion was collected. The solvents were removed, and the solid was recrystallized from CH₂Cl₂/MeOH, yielding 2.5 g of dark green solid *zDIP2* (12.3 % total yield). The obtained *zDIP2* product was further purified by sublimation under high vacuum (10⁻⁵ torr) using gradient temperature zones of 220 °C/160 °C/120 °C. ¹H NMR (400 MHz, CDCl₃): δ ppm 6.92 (s, 4H), 6.46-6.43 (m, *J* = 4.25 Hz, 4H), 6.13 (d, *J* = 3.94 Hz, 4H), 2.37 (s, 6H), 2.14 (s, 12H), 2.11 (s, 12H) matches well with published data.⁵⁰

Bis(1,3,7,9-tetramethyl-5-mesityldipyrrinato) zinc (zDIP3). 3.0 g of orange-red solid (13 % total yield). The obtained *zDIP3* was further purified by sublimation under high vacuum (10⁻⁵ torr) using 230 °C/160 °C/120 °C gradient temperature zones. ¹H NMR (500 MHz, CDCl₃): δ ppm 6.93 (s, 4H), 5.91 (s, 4H), 2.35 (s, 6H), 2.12 (s, 12H), 2.04 (s, 12H), 1.31 (s, 12H). ¹³C NMR (125 MHz, CDCl₃): δ ppm 155.90, 143.63, 143.15, 137.35, 136.22, 135.57, 134.54, 128.73, 119.56, 21.21, 19.26, 16.12, 14.83. HSMS: calcd for C₄₄H₅₁N₄Zn (MH⁺): 699.3400, found: 699.3407. C, H, N elemental analysis for C₄₄H₅₁N₄Zn: calcd (%) C (75.47), H (7.20), N (8.00); found (%) C (75.84), H (7.27), N (8.06).

Bis(2,8-diethyl-1,3,7,9-tetramethyl-5-mesityldipyrrinato) zinc (zDIP4). 0.8 g of orange-red solid (8 % total yield). The obtained *zDIP4* was further purified by sublimation under high vacuum (10⁻⁵ torr) using 250 °C/160 °C/120 °C gradient temperature zones. ¹H NMR (500 MHz, CDCl₃): δ ppm 6.92 (s, 4H), 2.36 (s, 6H), 2.25 (q, *J* = 7.40 Hz, 8H), 2.11 (s, 12H), 1.97 (s, 12H), 1.19 (s, 12H), 0.91 (t, *J* = 7.49 Hz, 12H). ¹³C NMR (500 MHz, CDCl₃): δ ppm 154.68, 142.03, 137.19, 137.10, 137.03, 136.00, 134.17, 130.66, 128.55, 21.24, 19.47, 17.92, 15.25, 14.35, 11.75. HSMS: calcd for C₅₂H₆₇N₄Zn (MH⁺) 811.4652, found 811.4658. CNH analysis for C₅₂H₆₆N₄Zn: calcd (%) C (76.87), H (8.19), N (6.90); found C (76.98), H (8.35), N (6.97).

Synthesis of heteroleptic complexes *zDIP2'* and *zDIP3'*. Representative procedure for *zDIP2'* is the following.

Zinc(1,9-dimethyl-5-mesityldipyrinato)(2,2,6,6-tetramethyl-3,5-heptanedionato) (*zDIP2'*).

Concentrated HCl (4 drops) was added to a solution of *zDIP2* (96 mg, 0.149 mmol) in 15 ml dichloromethane. The reaction mixture was rigorously shaken for 30 seconds, then washed with brine (2 times), and Na₂CO₃ solution (2 times). The obtained solution of ligand in dichloromethane was dried over anhydrous Na₂CO₃ and filtered. The dried dipyrin ligand was used without further purification.

A solution of bis-(2,2,6,6-tetramethyl-3,5-heptanedionato)zinc, Zn(dpm)₂ (150 mg, 0.347 mmol) in a mixture of dichloromethane/methanol (40/40 ml) was prepared, and slowly added to a solution of the dipyrin ligand in 15 ml dichloromethane over the course of 5 minutes while stirring. The reaction mixture became brightly emissive upon addition of Zn(dpm)₂. To prevent disproportionation of *zDIP2'*, the solvents were immediately removed under reduced pressure after addition of Zn(dpm)₂, yielding an orange red solid. The obtained orange solid was dissolved in 10 ml dichloromethane, and 15 ml of methanol was layered on top. This solution was stored for 2 days at -5 °C. Two distinct types of red crystals were subsequently formed; large orange red crystals (heteroleptic complex) and small cubic dark red crystals (homoleptic complex). The large orange red crystals were manually separated under a microscope, yielding 18 mg (9.6%) of heteroleptic complex *zDIP2'*. The obtained crystals were suitable for crystal structure determination by X-ray diffraction. Unlike the homoleptic complex *zDIP2*, the heteroleptic product *zDIP2'* is highly emissive in dichloromethane under UV-lamp illumination. ¹H NMR (400 MHz, CDCl₃, ppm): 6.89 (s, 2H), 6.42–6.35 (m, 2H), 6.15–6.10 (m, 2H), 5.83–5.80 (m, 1H), 2.35 (s, 3H), 2.23 (s, 6H), 2.14 (s, 6H), 1.19 (s, 18H). ¹³C NMR (400 MHz, CDCl₃, ppm): 203.52, 158.63, 143.85, 138.78, 136.86, 136.81, 135.34, 131.87, 127.41, 116.86, 89.60, 41.73, 28.40, 21.09, 20.06, 16.79. HSMS: calcd for C₃₁H₄₁N₂O₂Zn (MH⁺): 537.2454, found: 527.2463.

Zinc(1,3,7,9-tetramethyl-5-mesityldipyrinato)(2,2,6,6-tetramethyl-3,5-heptanedionato) (*zDIP3'*).

zDIP3' was synthesized using a procedure similar to that used to prepare *zDIP2'*. An orange solid mixture of heteroleptic and homoleptic complexes was obtained. Unlike the weakly emissive solid of other zinc dipyrins, this orange solid mixture has very bright yellow emission under UV-illumination. The

heteroleptic complex was separated from the homoleptic one by sublimation under high vacuum (10^{-5} torr) using 170 °C/120 °C/50 °C gradient temperature zones (note that *zDIP3* sublimes at the higher temperature of 230 °C, see above), yielding of *zDIP3'* (50% yield). A suitable crystal from the sublimed solid was used for crystal structure determination. ^1H NMR (400 MHz, CDCl_3 , ppm): 6.91 (s, 2H), 5.92 (s, 2H), 5.79 (s, 1H), 2.33 (s, 3H), 2.13 (s, 12H), 1.28 (s, 6H), 1.18 (s, 18H). ^{13}C NMR (400 MHz, CDCl_3 , ppm): 203.25, 155.90, 144.19, 144.06, 137.46, 135.83, 135.71, 134.87, 128.75, 119.62, 89.46, 41.65, 28.38, 21.19, 19.68, 16.48, 14.81. HSMS: calcd for $\text{C}_{33}\text{H}_{45}\text{N}_2\text{O}_2\text{Zn}$ (MH^+): 565.2767, found: 565.2764.

Global Analysis of femtosecond Transient Absorption Spectra:

The transient absorption spectra of *zDIP1-3* indicate that compared to *zDIP1*, the population from initially formed S_1 state evolves faster to CT state for both *zDIP2* and *zDIP3*. In addition, the rate for formation of CT state and its subsequent relaxation were found to be dependent on the polarity of the surrounding medium. To quantify the rate of decay of these states in different polarity solvents, TA spectra were fit with a linear decomposition model described elsewhere in detail.¹ In brief, the signal can be described by:

$$S(\lambda, t) = \sum_n C_n(t) \sigma_n(\lambda) \quad (\text{S1})$$

where the time dependent TA signal, $S(\lambda, t)$, can be decomposed into a set of time independent species associated difference spectra (SADS), $\sigma_n(\lambda)$, and time dependent amplitudes, $c_n(t)$. Each SADS corresponds to the characteristic TA spectrum of an excited configuration of the system and consist of both positive features due to excited state absorption and negative features due to stimulated emission and ground state bleach. $c_n(t)$ is calculated assuming that the evolution of the initially excited population is governed by a series of sequential first order rate processes.

The kinetic model described in the main paper (Figure 9) was used to fit all the femtosecond transient absorption spectra. Based on the polarity of the solvents used, they were categorized as

1) nonpolar (cyclohexane), 2) weakly polar (toluene) and 3) polar (dichloromethane and acetonitrile). Depending on the solvent category different transfer matrices, K_{ij} are used for the kinetic model:

$$\text{Category 1) } K_{ij} = [k_{11}], \quad \text{Category 2) } K_{ij} = \begin{bmatrix} k_{11} & k_{21} \\ k_{12} & k_{22} \end{bmatrix}, \quad \text{Category 3) } K_{ij} = \begin{bmatrix} 0 & 0 \\ k_{12} & k_{22} \end{bmatrix}$$

Here k_{11} and k_{22} represent the first order rates for the decay of the S_1 excited state and the CT state, respectively. And k_{12} and k_{21} represent the first order transfer rates from S_1 excited state to the CT state and from the CT state to the S_1 excited state. The solvent polarity dependent data for *zDIP1* (shown in Figure 8) was fitted with this model and the SADS required to model each of the data are shown in Figure S18 (a,c,e,g). These SADS are the characteristic transient spectral signature for the initially populated S_1 excited state (σ_1) and subsequently formed CT state (σ_2). The corresponding fits to the time slices of the ground state bleach and CT state induced absorption are also shown in Figure S18 (b,d,f,h).

Excited State Dynamics of *zDIP2* and *zDIP3*:

Figure S19 and S21 shows the solvent polarity dependent TA spectra for *zDIP2* and *zDIP3*, respectively. In cyclohexane, both *zDIP2* (Fig. S19a) and *zDIP3* (Fig. S21a) show similar dynamics to that observed for *zDIP1* in the main paper, however the relaxation of the S_1 excited state to the ground state for *zDIP3* is faster (~ 1.4 ns) compared to *zDIP1* (4.5 ns) and *zDIP2* (4.8 ns). This dramatic decrease in S_1 excited state lifetime for *zDIP3* is also consistent with the TCSPC results (shown in Fig. S23) and it is due to presence of higher non-radiative processes discussed in the main paper (Figure 5).

However in toluene, for both *zDIP2* (Fig. S19b) and *zDIP3* (Fig. S21b) over the time some population from initially formed S_1 state evolve to CT state (indicated by the induced absorption

growing at ~ 370 nm) and some relax back to the ground state (stimulated emission at ~ 525 nm remains till 1 ns). And so an equilibrium exists between the CT state and S_1 state similar to that observed in $zDIP1$ in the main paper. The forward and backward rate constants ($1/k_{CT}$ and $1/k_{CR}$) between the S_1 and the CT states obtained from the global analysis are 8.6 and 15.5 ps; 2.3 and 11.2 ps respectively for $zDIP2$ and $zDIP3$. Once formed, the CT state decays with a rate constant ($1/k_{rec}$) of 4.0 ns and 2.5 ns for $zDIP2$ and $zDIP3$, respectively. Unlike toluene, in polar solvents such as acetonitrile $zDIP3$ (Fig. S21c) evolves to CT state at a faster rate ($1/k_{CT} = 1$ ps) due to the stabilization of the CT states by the large solvation energy of the acetonitrile. The SADS and the fits for the time traces obtained from the modeling of the TA spectra using global analysis for $zDIP2$ and $zDIP3$ are shown in Figure S20 and S22, respectively.

Comparison between Spectro-electrochemistry and TA measurements of $zDIP1$:

The spectral assignment of $zDIP1$ anion is obtained from spectro-electrochemical reduction experiments in dichloromethane (Figure 7, main paper). This assignment is used to assign the induced absorption band at 517 nm from TA measurements (Figure 8, main paper). In Fig. S25 the two absorption profiles are overlaid to make a direct comparison between the two experiments. Although the peak at 517 nm matches perfectly, the bleach shape looks different between the two experiments. This is mainly due to the presence of an additional peak between 370-470 nm (encircled in green) in the spectro-electrochemical reduction experiments. The absence of this peak in TA data is probably because the molecule forms both a $zDIP1$ radical cation and radical anion in its excited state (as probed in TA experiment) whereas in the reduction experiments there is only $zDIP1$ radical anion present. We suspect that the total absorptions for the radical anion is obscured by the presence of radical cation, and the anion signal may be overwhelmed by the bleach signal which is doubled due to removal of two chromophores (one

forming the anion and the other forming the cation). Another possible reason could be a two electron reduction, *i.e.* reduction of both dipyrin ligands, in spectro-electrochemical experiments.

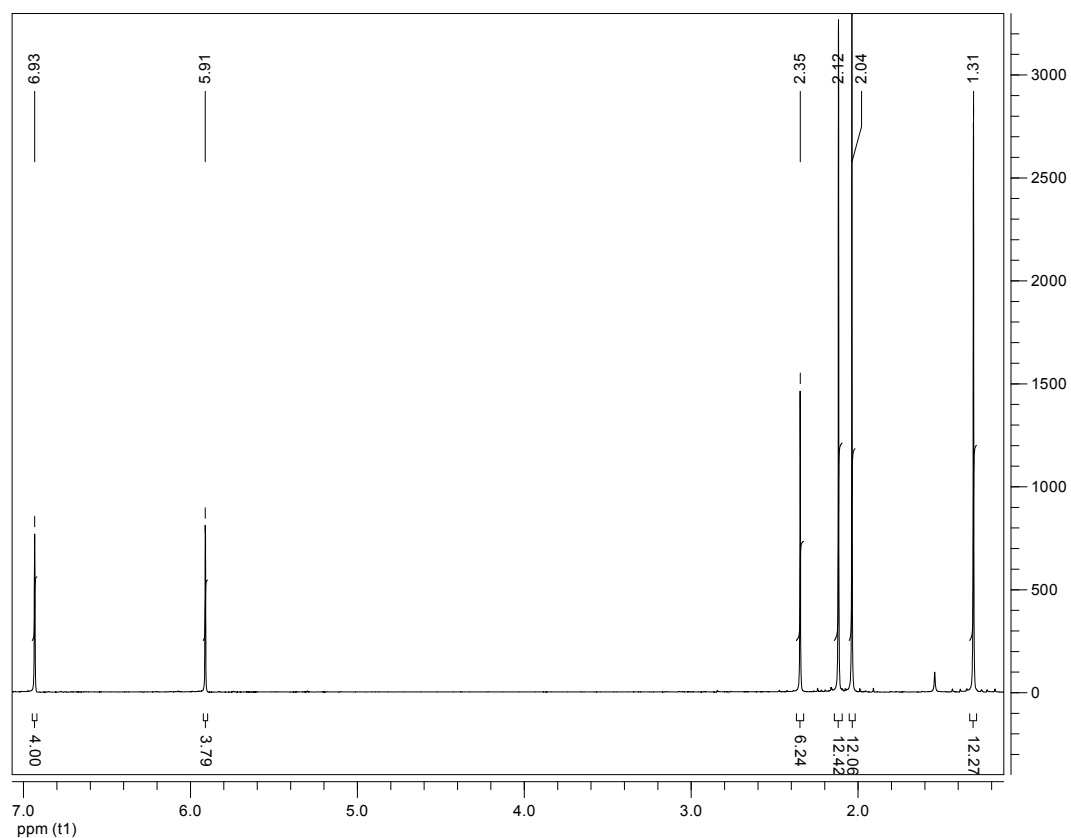


Figure S1. ^1H NMR of *zDIP3*.

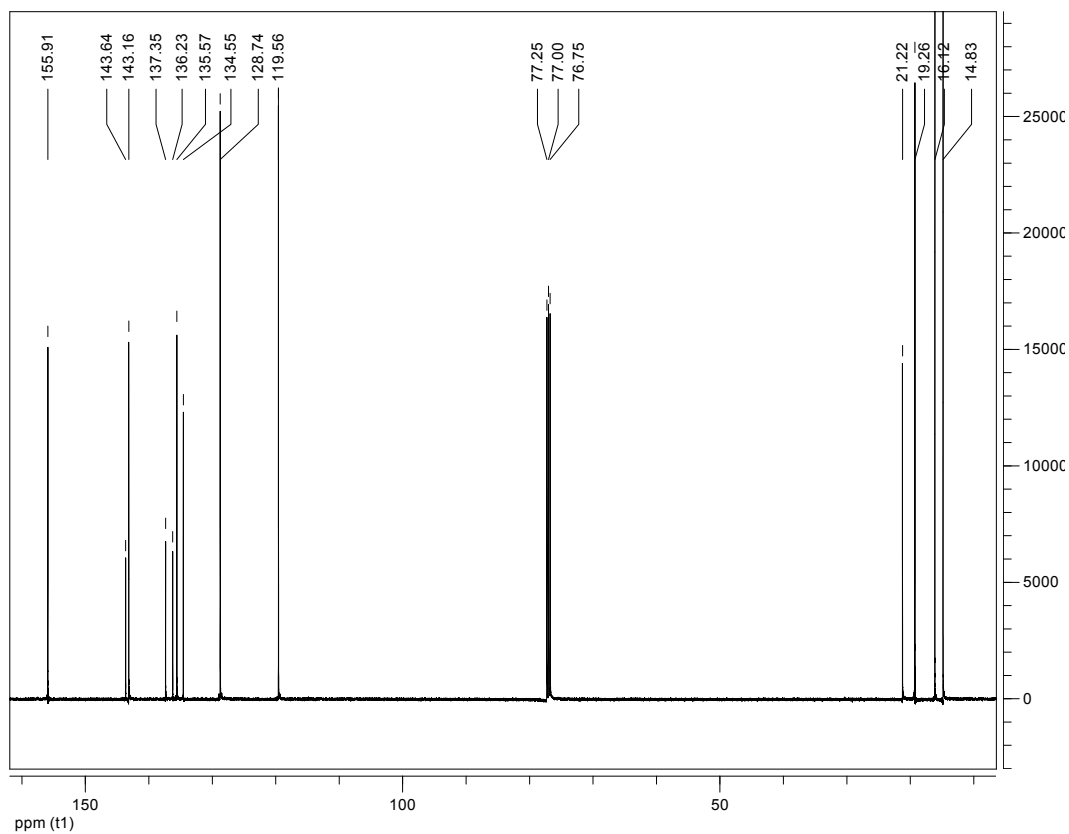


Figure S2. ^{13}C NMR of *zDIP3*.

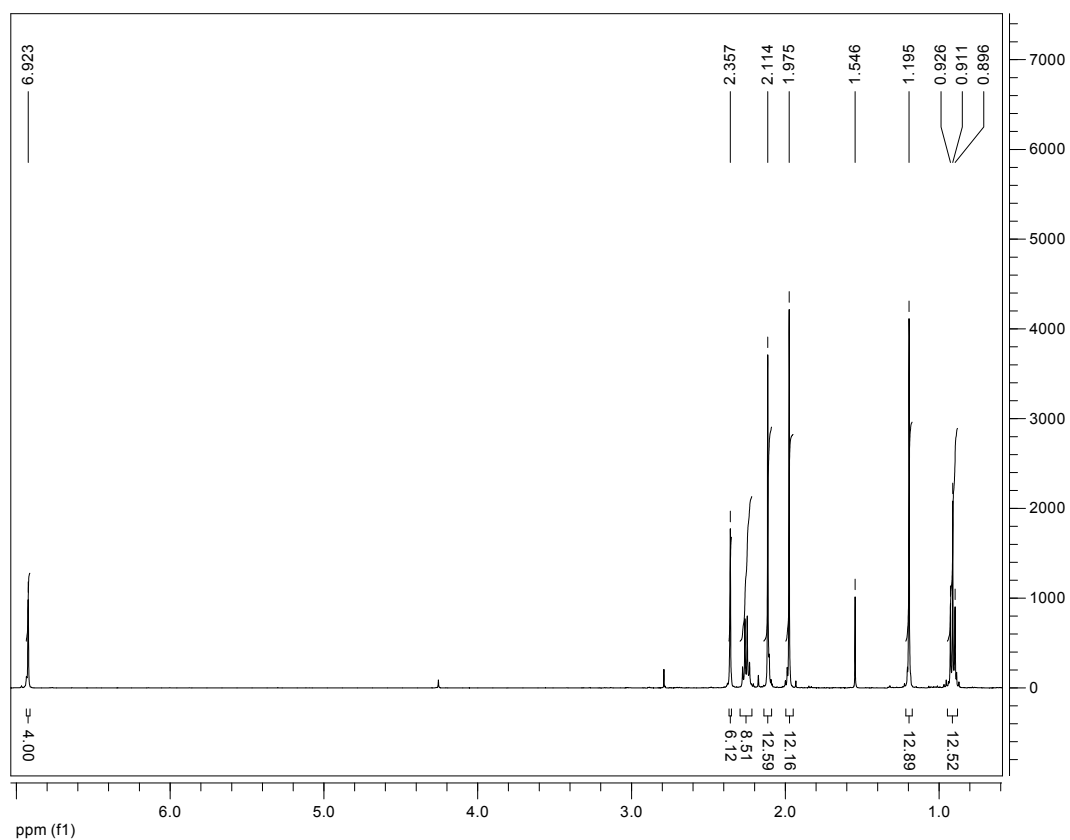


Figure S3. ¹H NMR of *zDIP4*.

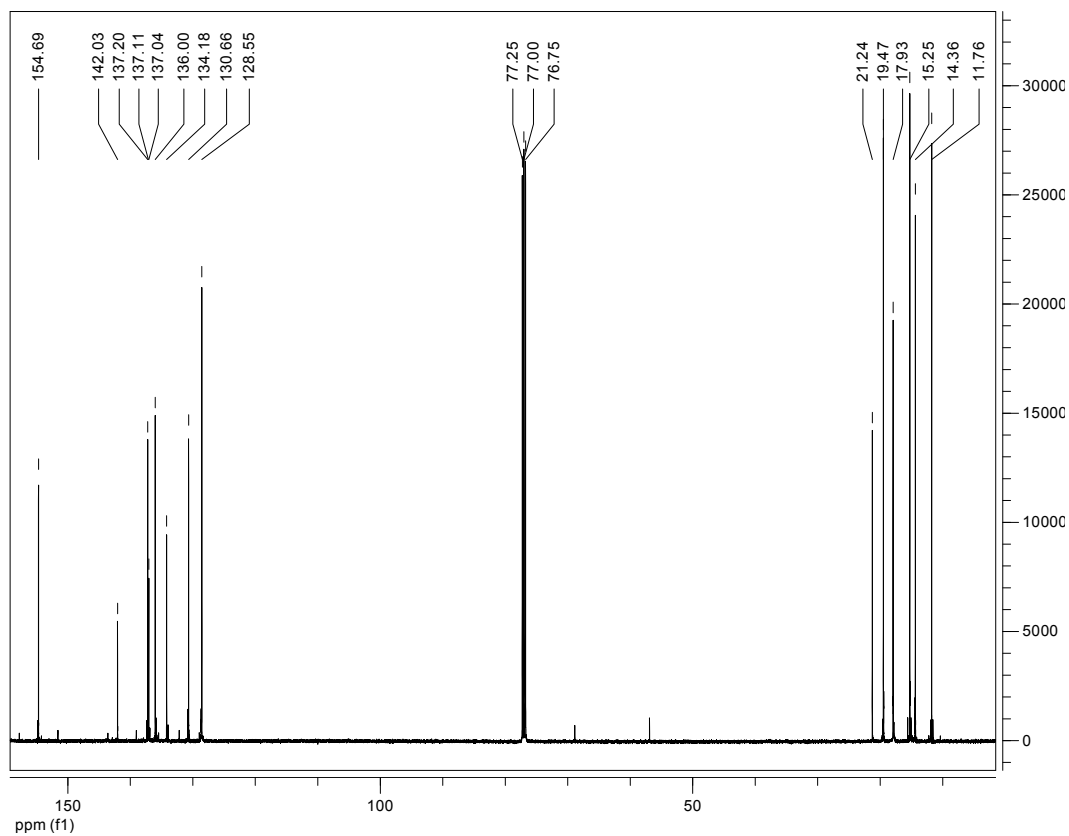
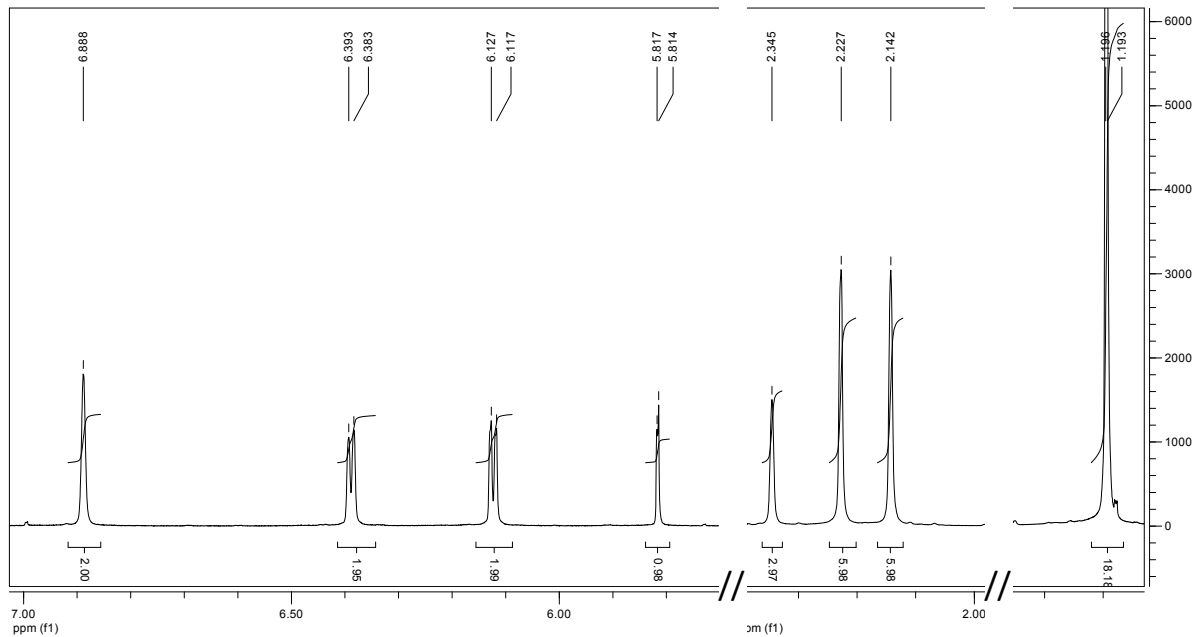


Figure S4. ^{13}C NMR of *zDIP4*

a)



b)

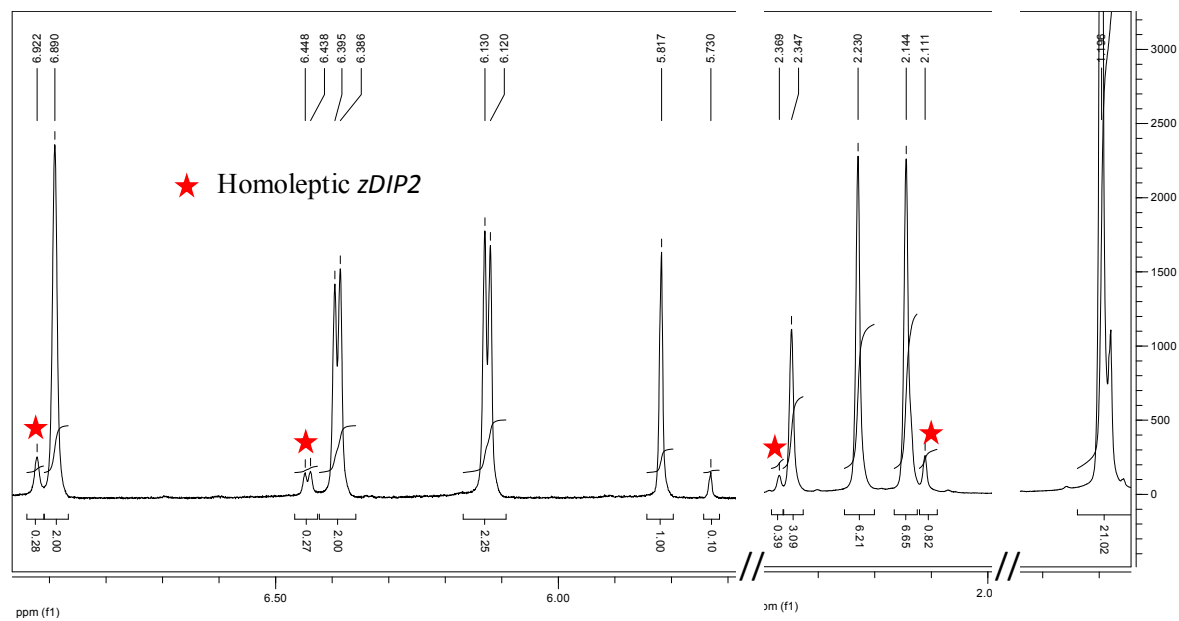


Figure S5. ^1H NMR of $z\text{DIP5}$ in CDCl_3 over time. (a) freshly prepared solution of $z\text{DIP5}$ and (b) solution in NRM tube after 4 hours, estimated molar ratio of heteroleptic:homoleptic complexes ($z\text{DIP5}$: $z\text{DIP2}$ = 15:1)

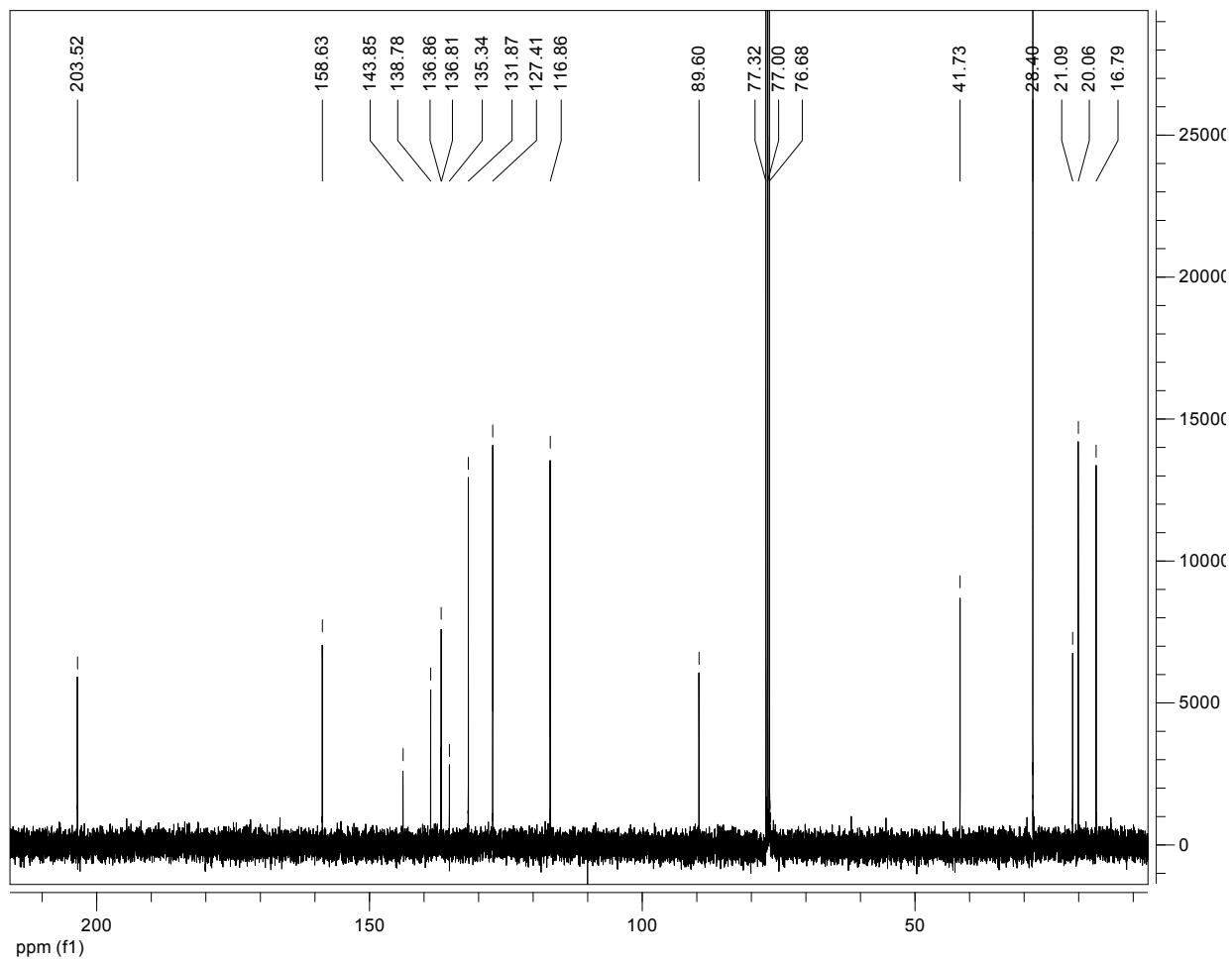


Figure S6. ¹³C NMR of *zDIP5* in CDCl₃.

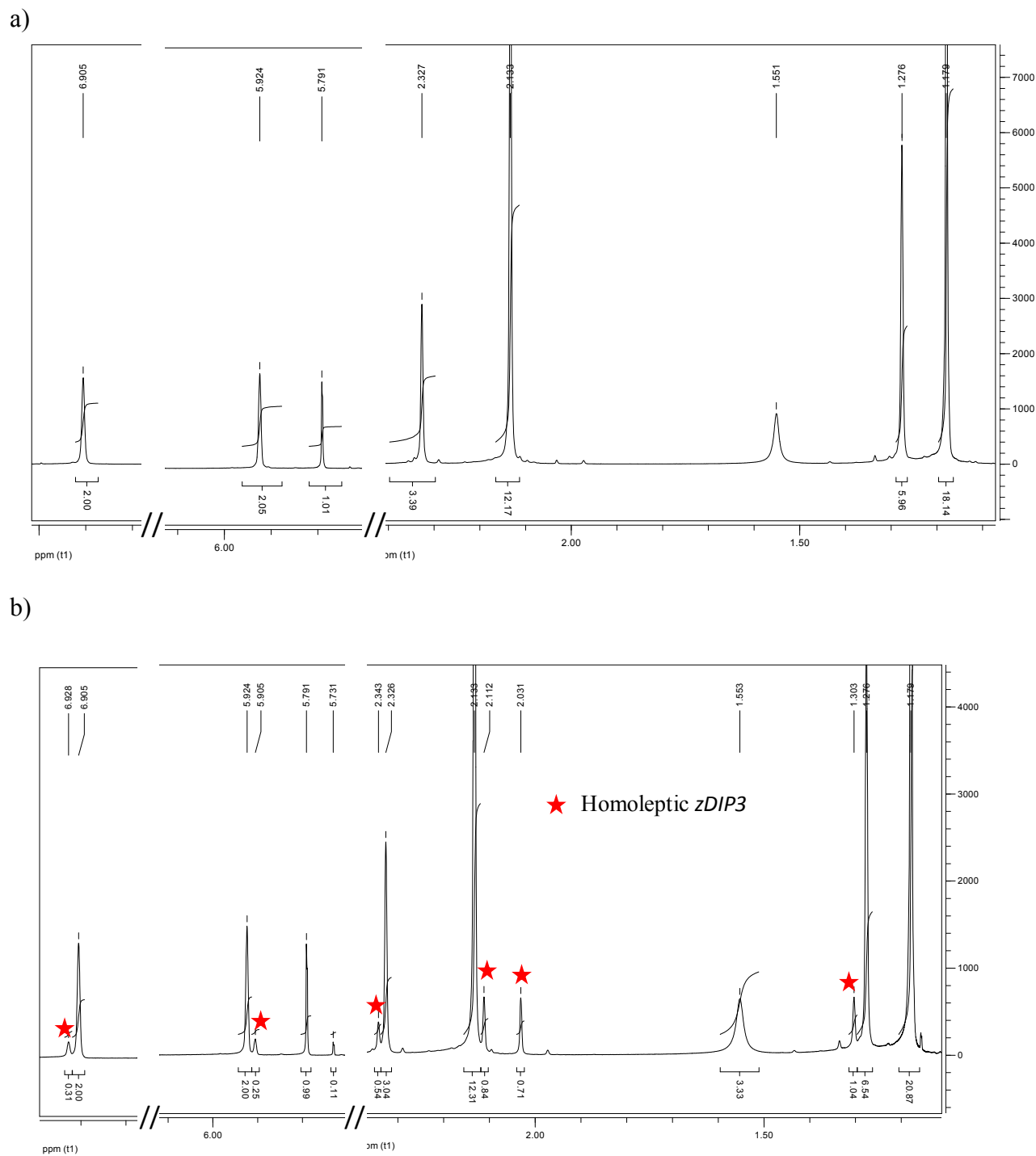


Figure S7. ^1H NMR of $z\text{DIP6}$ in CDCl_3 over time. (a) freshly prepared solution of $z\text{DIP6}$ and (b) solution in NRM tube after 8 hours, estimated molar ratio of heteroleptic:homoleptic complexes ($z\text{DIP6}$: $z\text{DIP3}$ = 13:1)

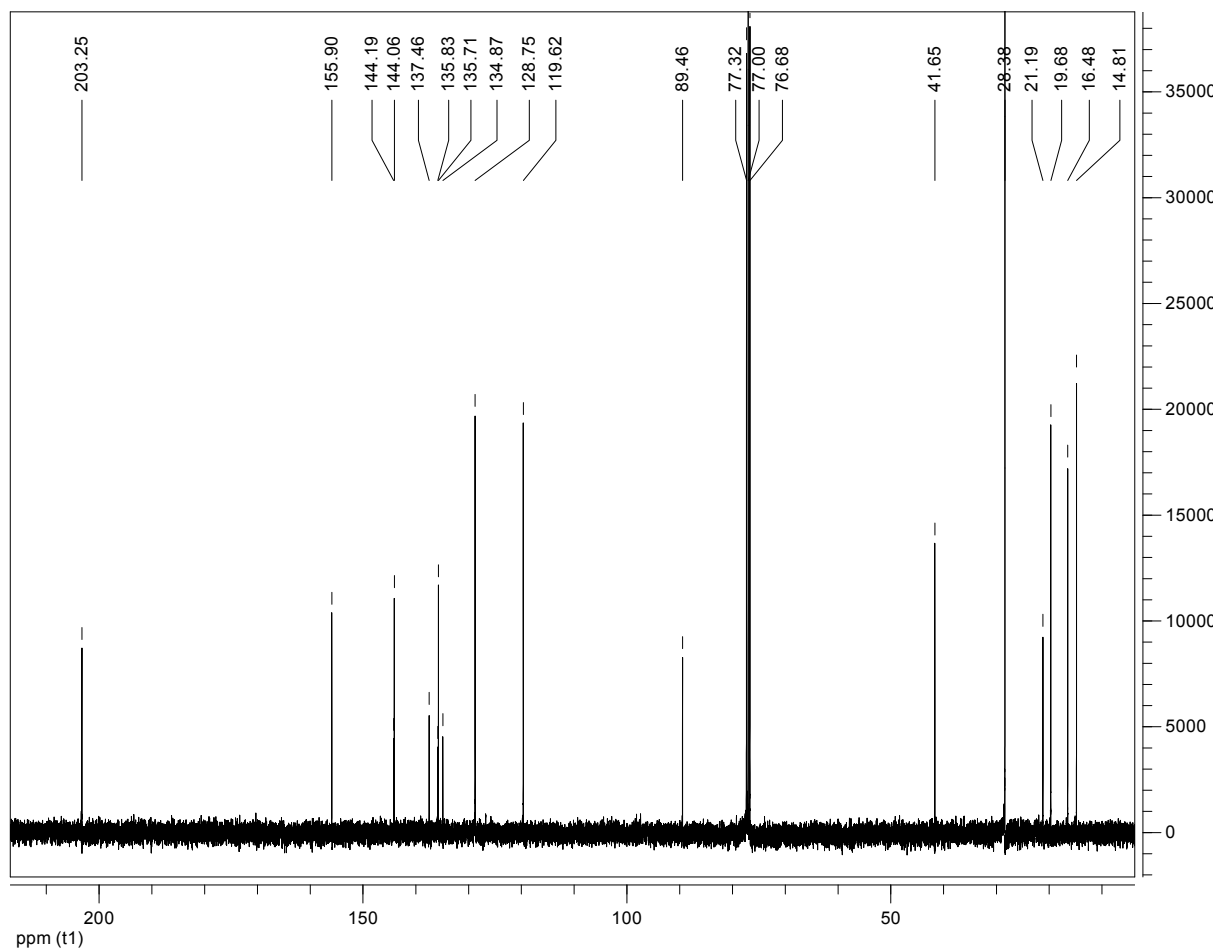


Figure S8. ¹³C NMR of *zDIP6* in CDCl₃.

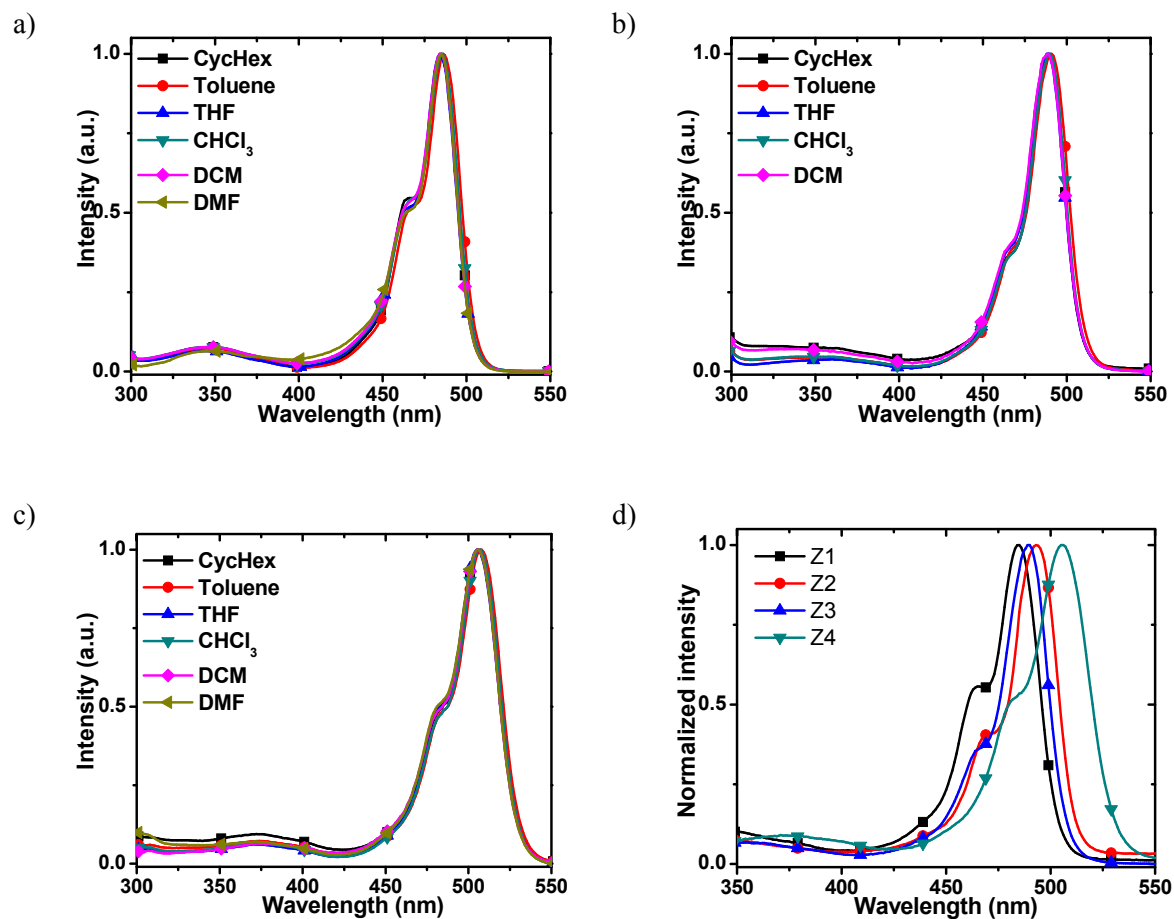


Figure S9. Absorption spectra in different solvents of (a) *zDIP1*, (b) *zDIP3*, (c) *zDIP4*; and (d) absorption spectra of *zDIP1-4* in cyclohexane.

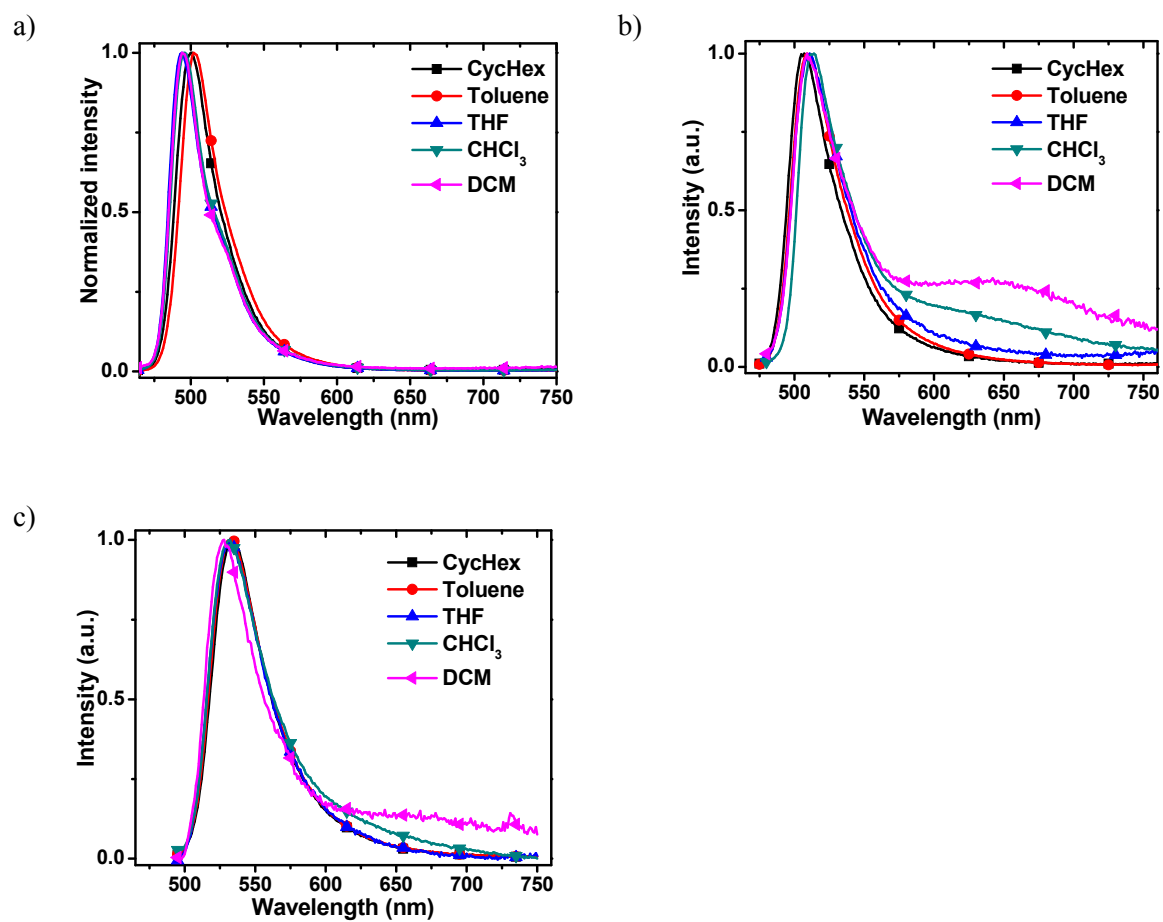


Figure S10. Normalized emission spectra in different solvents of (a) *zDIP1*, (b) *zDIP3* and (c) *zDIP4*.

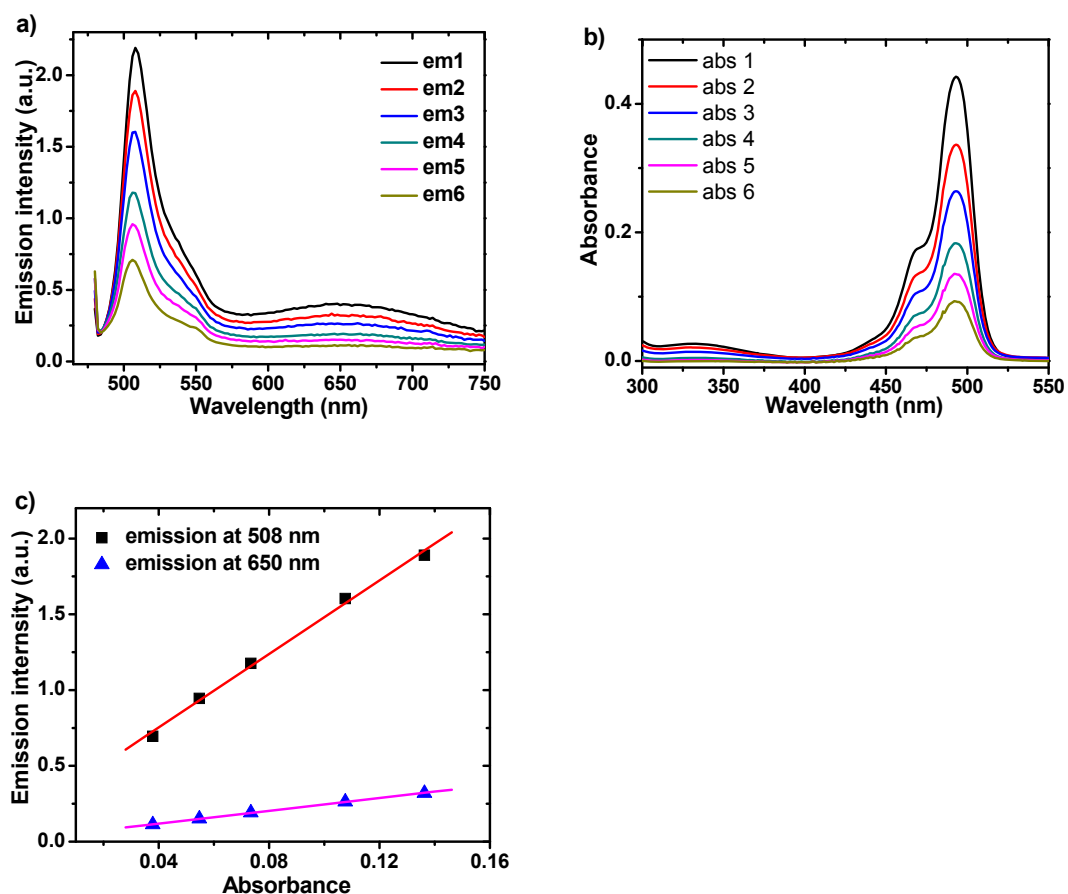


Figure S11. Emission and absorption intensities of *zDIP2* solution in dichloromethane at various concentrations. (a) emission spectra and (b) corresponding absorption spectra as concentration decreases; (c) emission intensities are plotted vs. absorption intensity, linear dependence of emission peaks at 508 and 650 nm excludes excimer formation in solution.

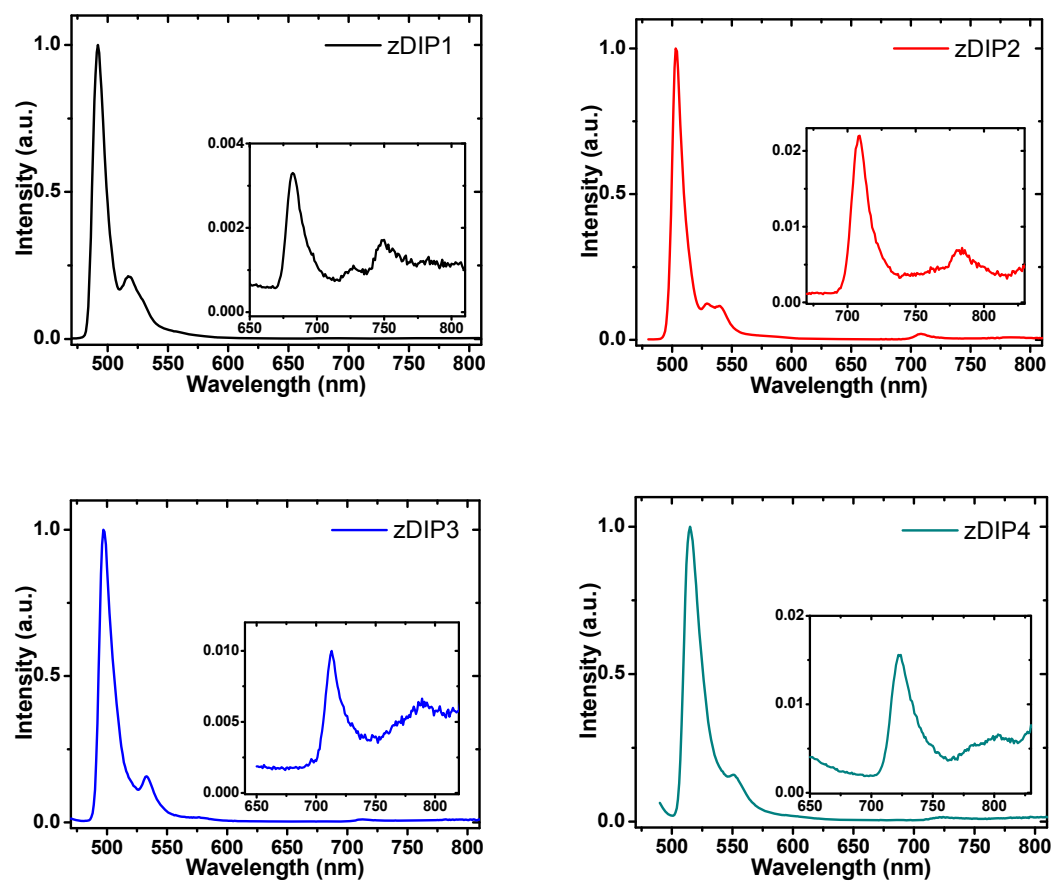


Figure S12. Emission spectra of *zDIP1-4* in 2-methyl tetrahydrofuran at 77K.

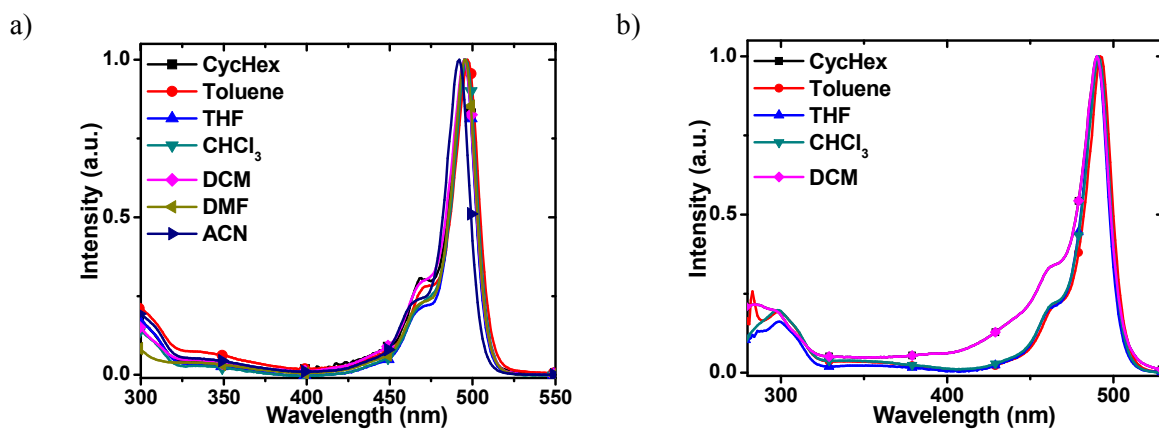


Figure S13. Absorption spectra of heteroleptic complexes (a) *zDIP5* and (b) *zDIP6* in different solvents.

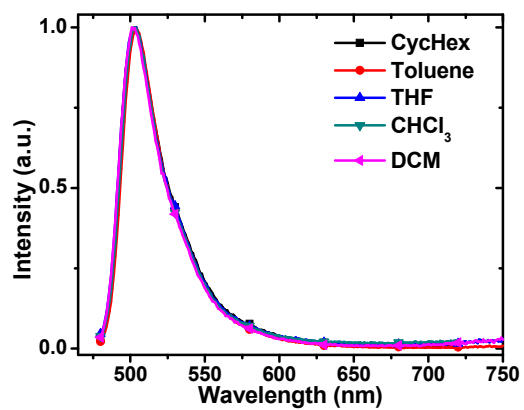


Figure S14. Emission spectra of *zDIP6* in different solvents.

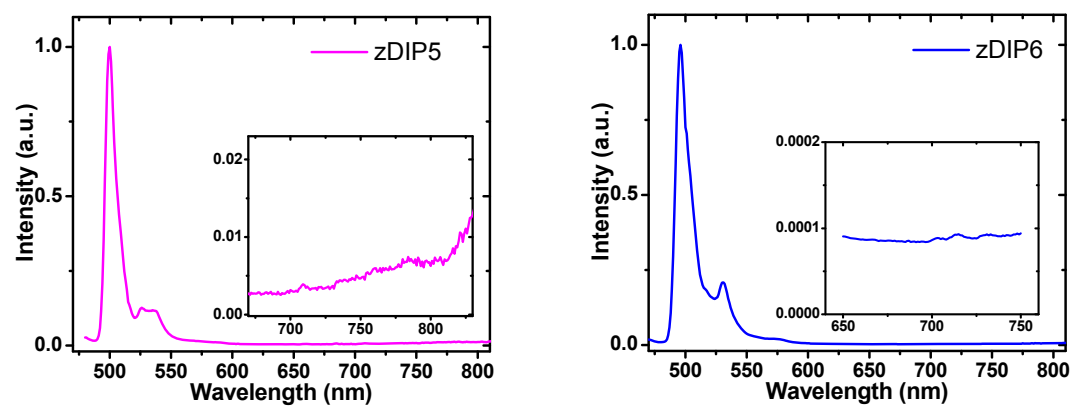


Figure S15. Emission spectra of *zDIP5* (left) and *zDIP6* (right) in 2-methyl tetrahydrofuran at 77K.

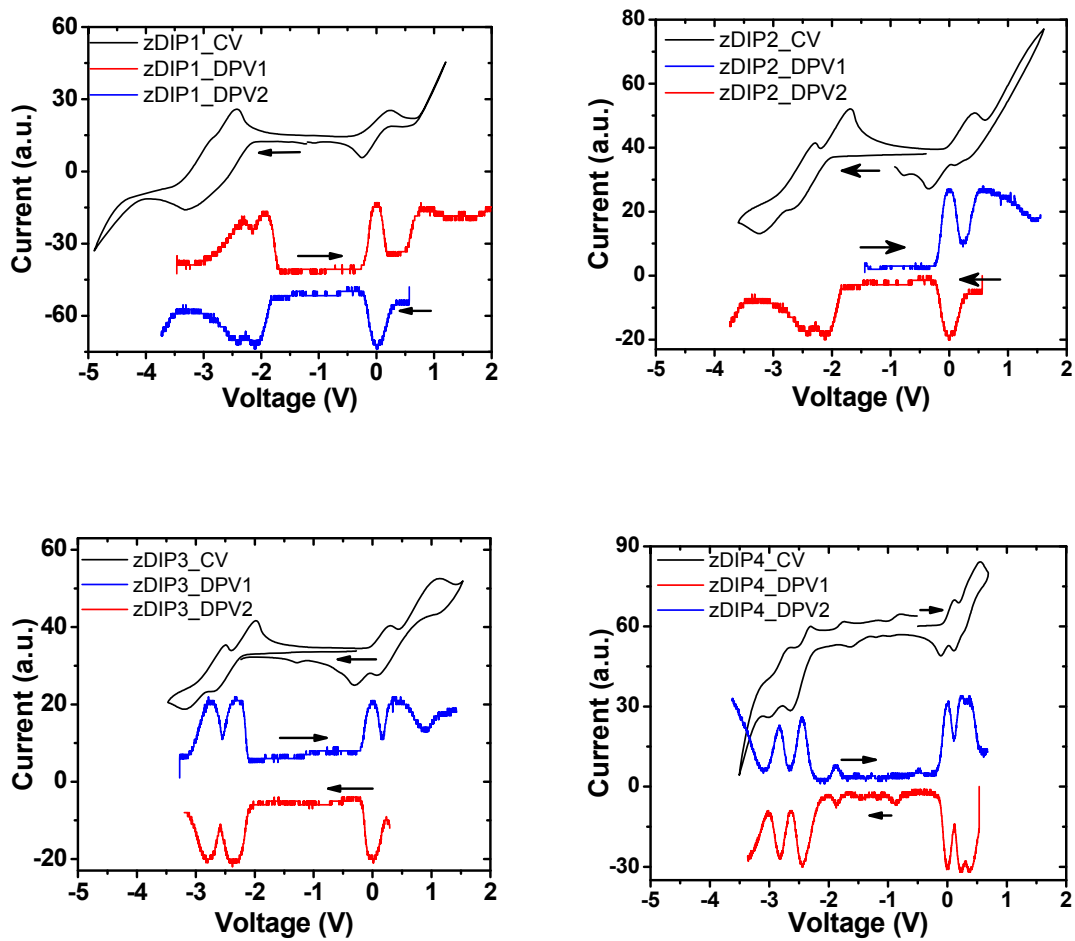


Figure S16. Electrochemical measurements of *zDIP1-4* in dry THF under N_2 , scan rate is 100 mV/s. Fc^+/Fc was used as internal standard.

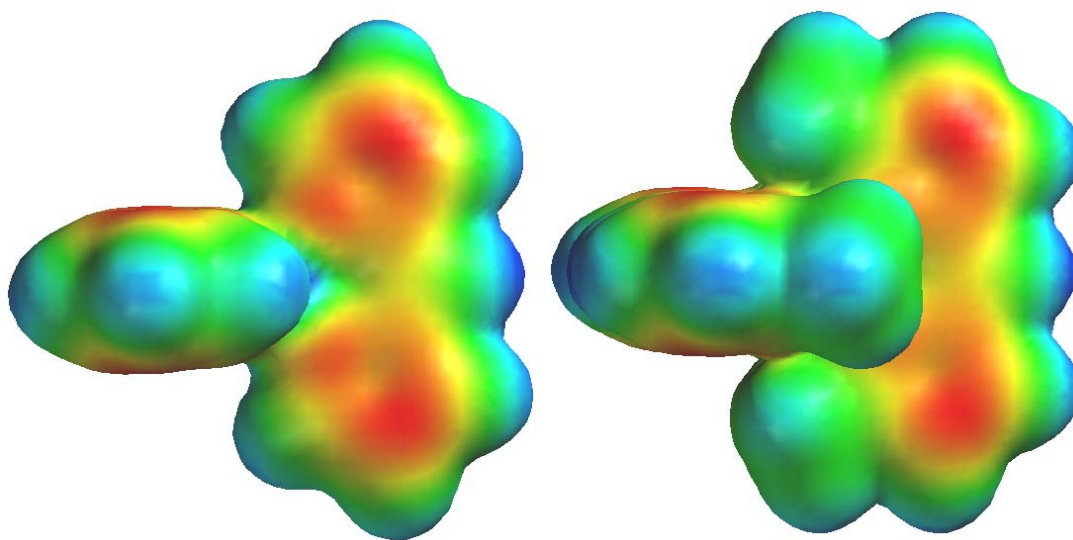


Figure S17. Electron density surfaces of *zDIP1* (left) and *zDIP2* (right) with D2d symmetry, performed at B3LYP/LACVP** level of theory. Mesityl group are omitted for simplicity of calculation.

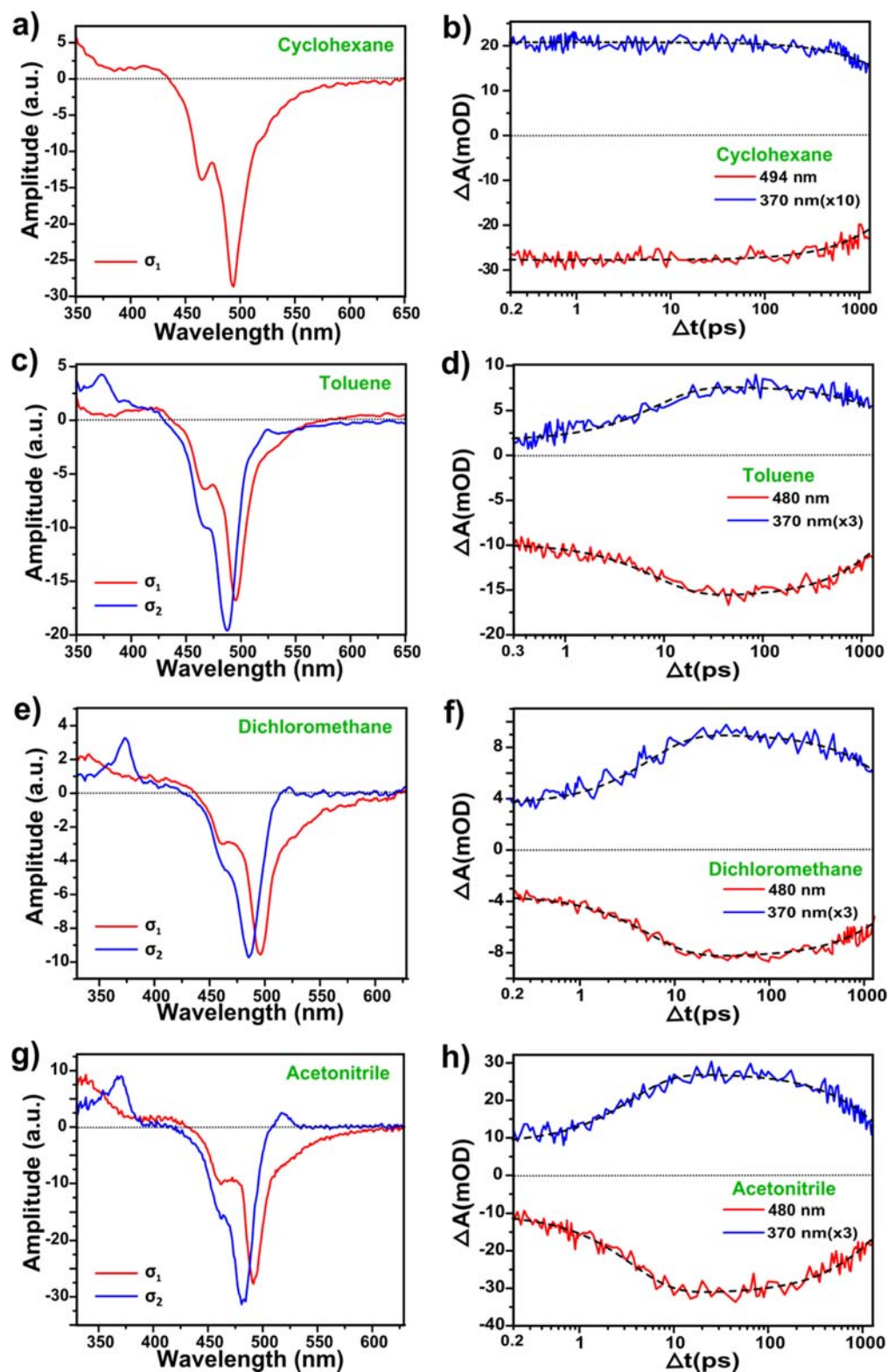


Figure S18: (a, c, e, g) SADS used to model the transient spectra of *zDIP1*. (b, d, f, h) The fits (black dashed) based on SADS analysis for the time slices taken through the ground state bleach (red) and spectral range indicative of CT state (blue).

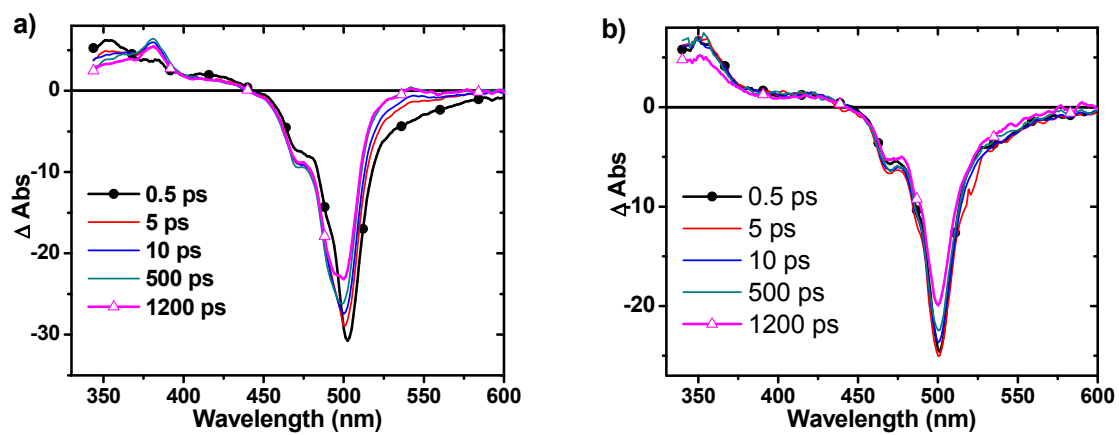


Figure S19. Transient absorption spectra of *zDIP2* in (a) toluene and (b) cyclohexane.

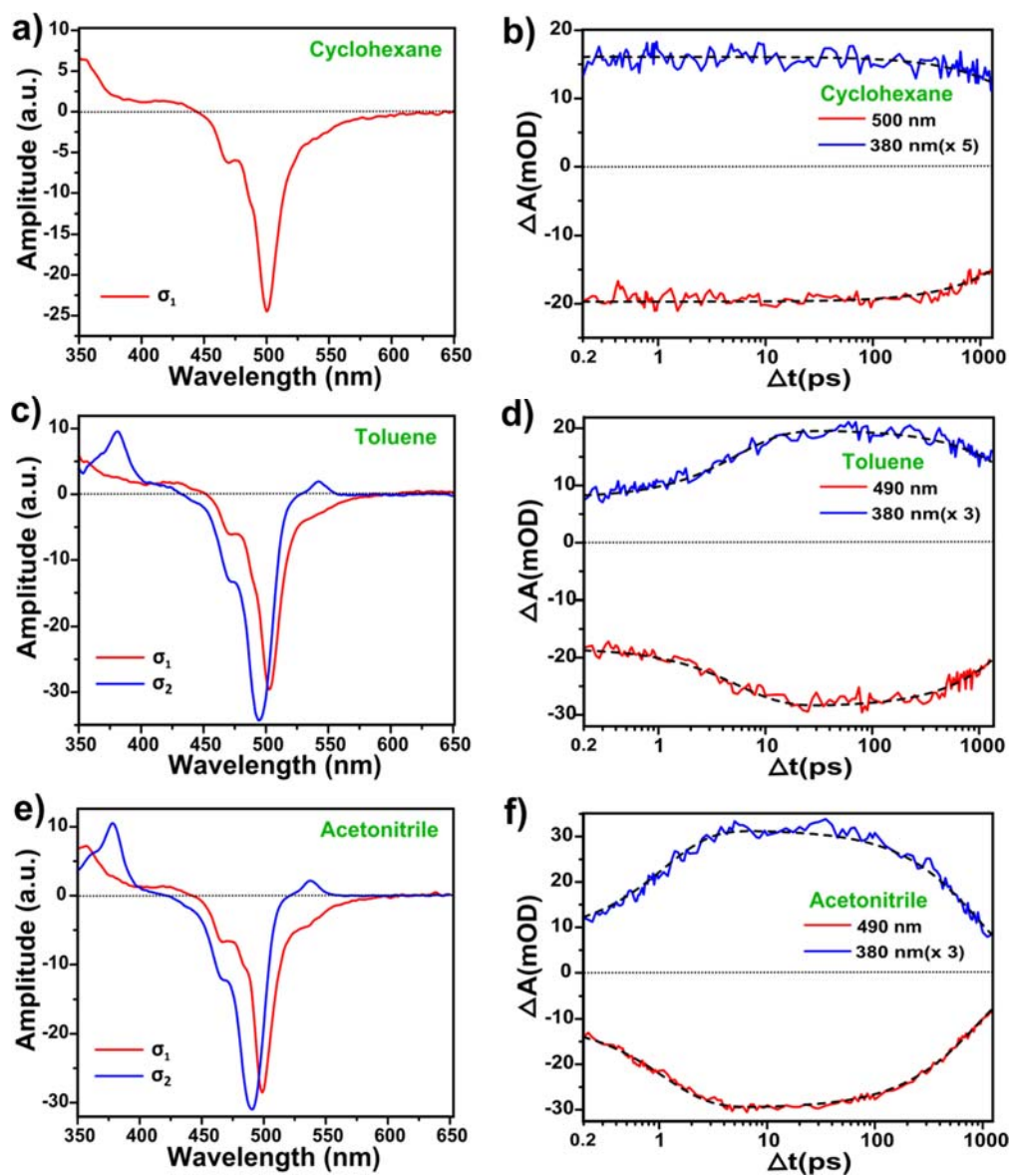


Figure S20: (a, c, e) SADS used to model the transient spectra of *zDIP2*. (b, d, f) The fits (black dashed) based on SADS analysis for the time slices taken through the ground state bleach (red) and spectral range indicative of CT state (blue).

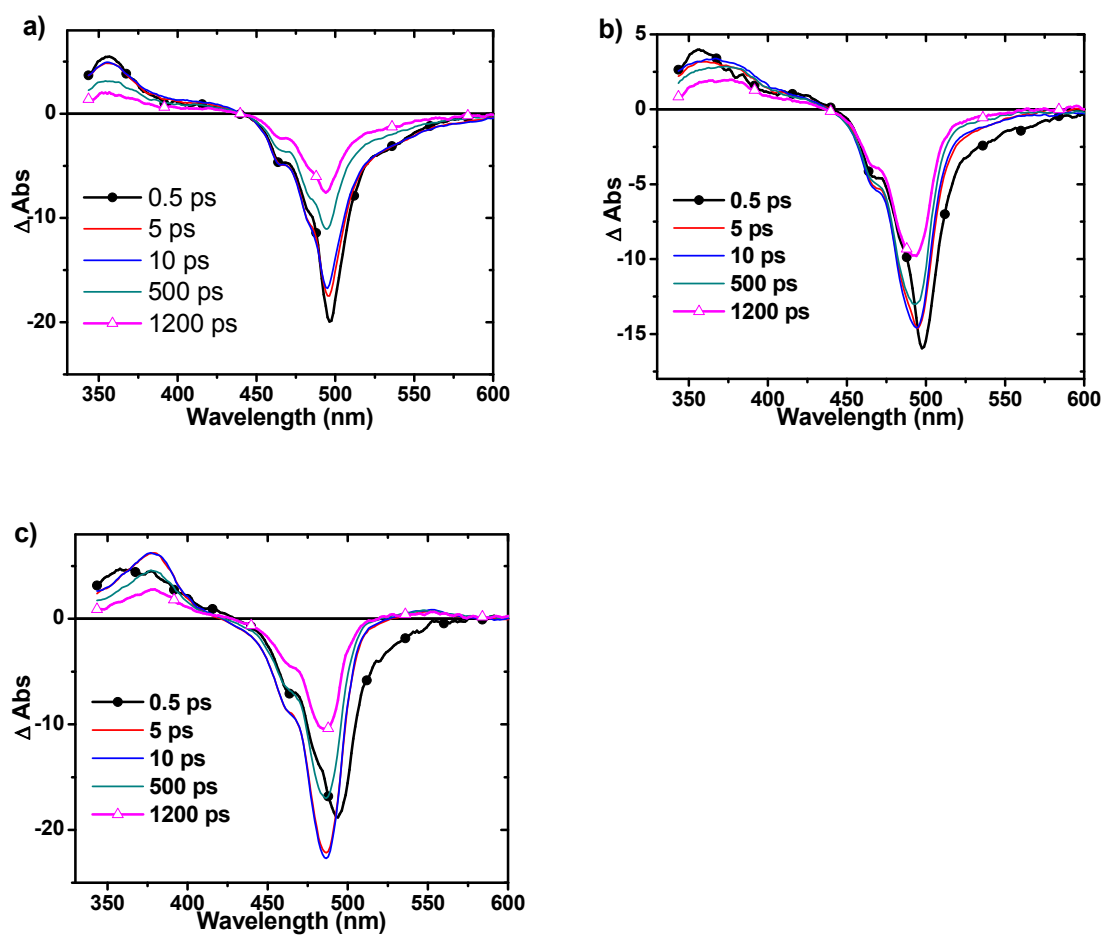


Figure S21. Transient absorption spectra of *zDIP3* in (a) Cyclohexane, (b) toluene and (c) acetonitrile.

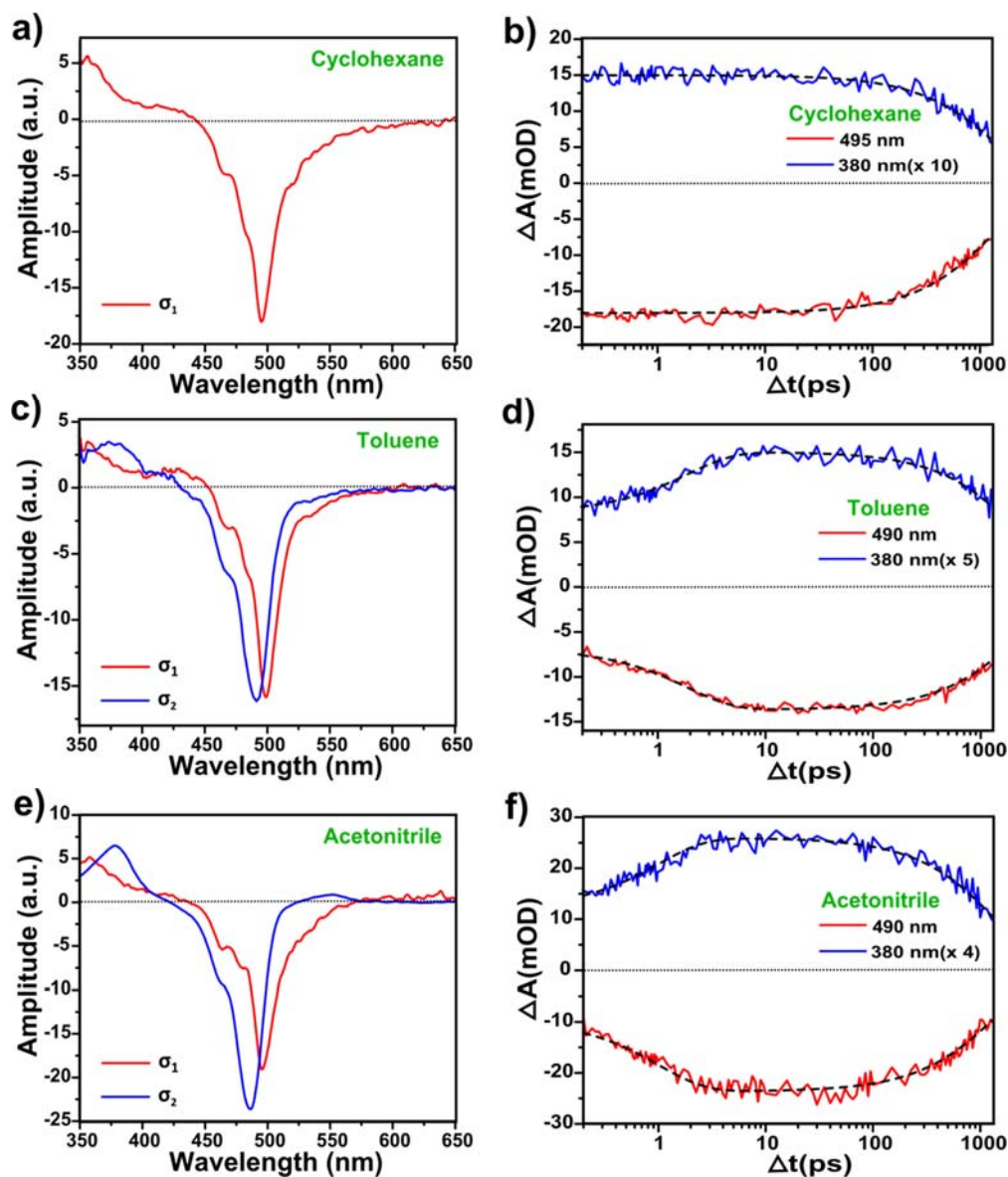


Figure S22: (a, c, e) SADS used to model the transient spectra of *zDIP3*. (b, d, f) The fits (black dashed) based on SADS analysis for the time slices taken through the ground state bleach (red) and spectral range indicative of CT state (blue).

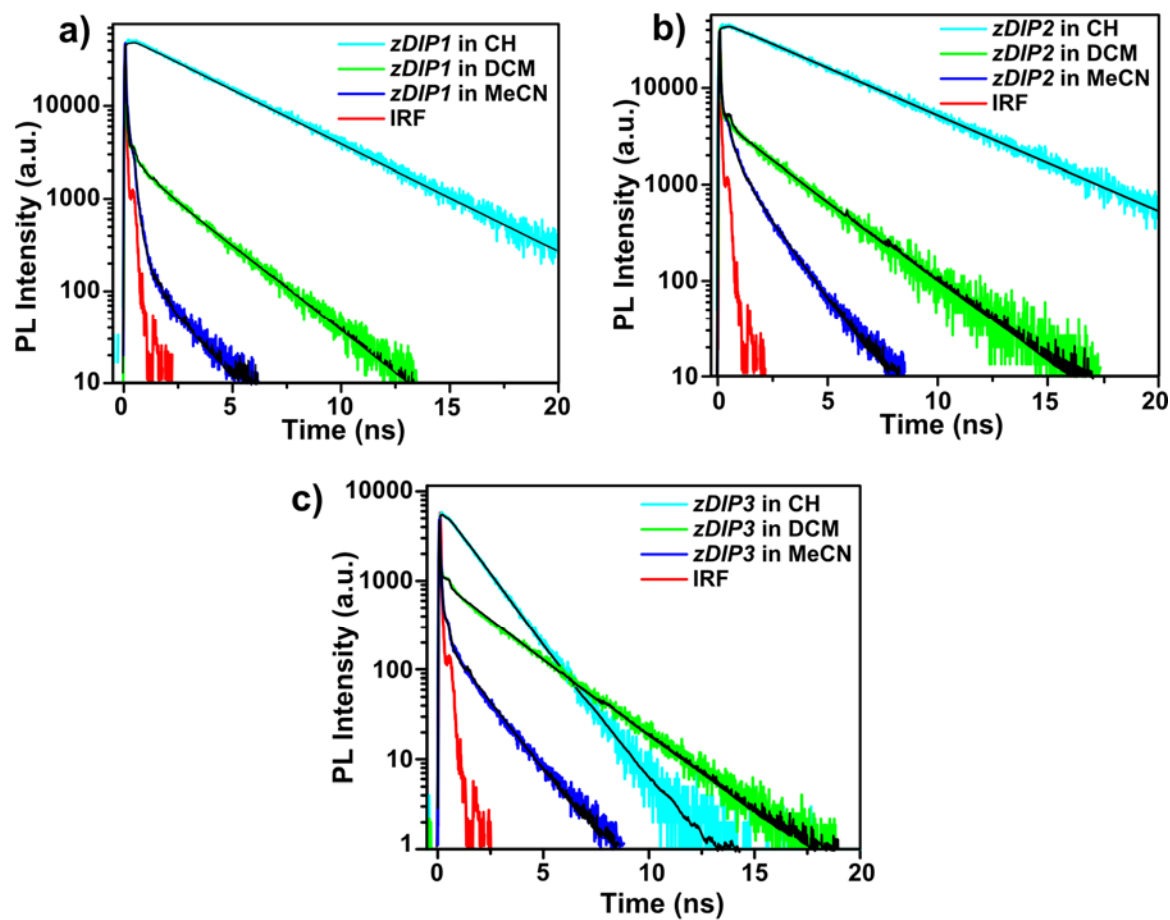


Figure S23: Normalized photoluminescence (PL) measurements of a) *zDIP1*, b) *zDIP2* and c) *zDIP3* in various polarity solvents. The emission is collected at 520 nm following excitation with 500 nm. The instrument response function (FWHM \sim 22 ps) is also shown in red. The black lines are the fit to the PL measurements with exponential(s) (amplitudes and time constants are shown in table S14).

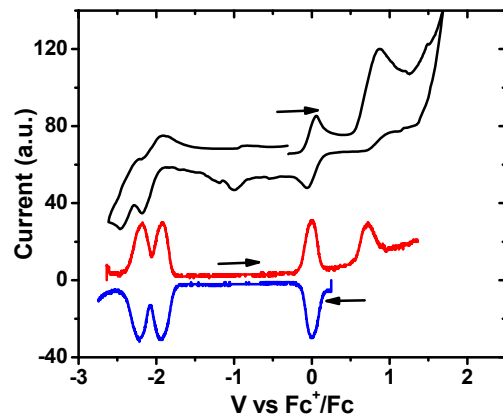


Figure S24. Electrochemical measurement of *zDIP1* in DCM, *zDIP1* undergoes irreversible oxidation and two reversible reductions.

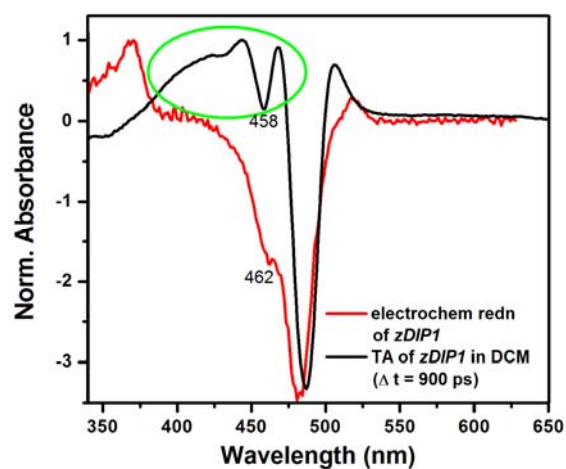
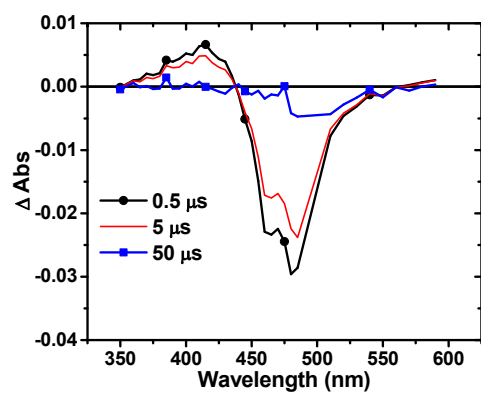


Figure S25. Spectral lineshape comparison between spectro-electrochemical reduction and TA experiments on *zDIP1* in DCM. The encircled portion in green shows the peak responsible for the difference.

a)



b)

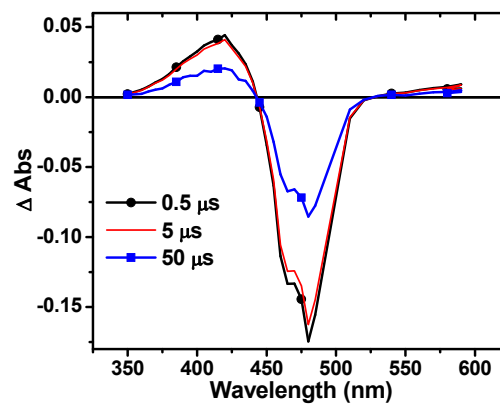


Figure S25. Microsecond transient absorption spectra of *zDIP1* (a) in cyclohexane and (b) in toluene

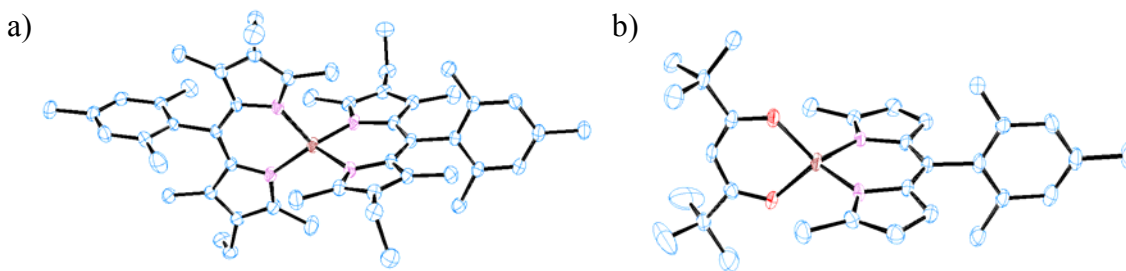


Figure S26. ORTEP diagrams of (a) *zDIP4* and (b) *zDIP5* at 50% probability level. H atoms are omitted for clarity.

Table S1. Photophysical properties of homoleptic and heteroleptic zinc dipyrin complexes in different solvents at room temperature.

Solvents	λ_{abs} (max/nm)	fwhm _{ab} (cm ⁻¹)	λ_{em} (max/nm)	fwhm _{em} (cm ⁻¹)	$\Delta\nu_{\text{ab-em}}$ (cm ⁻¹)	QE (%)	τ (ns)	k _r (ns ⁻¹)	k _{nr} (ns ⁻¹)
<i>zDIP1</i> CycHex	484	1530	501	1260	638	46.5	4.3	0.11	0.12
Toluene	486	1443	503	1256	659	33.3	3.0	0.11	0.22
THF	484	1437	494	1231	406	2.7	2.6 ^(a)	0.01	0.37
CHCl ₃	485	1483	496	1218	426	2.2	-	-	-
DCM	485	1471	495	1131	429	1.7	2.1 ^(b)	-	-
ACN	481	1423	490	1180	396	< 0.1	1.7 ^(b)	-	-
<i>zDIP2</i> CycHex	493	983	506	944	501	66.0	4.8	0.14	0.07
Toluene	495	1022	509	959	567	19.0	3.9	0.05	0.21
THF	493	1016	507	1013	586	0.9	2.9 ^(a)	0.003	0.34
CHCl ₃	494	1083	509	1013	592	0.5	2 ^(a)	-	-
DCM	493	1074	508 (650)	1108	706	< 0.1	2.5 ^(b) (2.2 ^(c))	-	-
ACN	490	1056	508	1494	736	-	1.4 ^(b)	-	-
<i>zDIP3</i> CycHex	489	1036	507	1500	676	16.3	1.5	0.11	0.56
Toluene	491	1102	509	1523	736	13.8	2.1	0.07	0.41
THF	489	1092	511	1576	902	2.0	2.8 ^(a)	0.007	0.35
CHCl ₃	490	1057	513	1494	915	0.5	-	-	-
DCM	488	1127	509 (653)	1591	819	< 0.1	2.4 ^(b) (2.5 ^(c))	-	-
<i>zDIP4</i> CycHex	506	1393	533	1480	1026	17.4	1.9	0.09	0.43
Toluene	508	1323	533	1565	920	13.4	2.4	0.06	0.36

THF	505	1432	532	1604	982	2.6	2.6 ^(a)	0.01	0.37
CHCl ₃	507	1296	532	1632	917	0.7	-	-	-
DCM	506	1403	528 (674)	1503	831	< 0.1	-	-	-
<hr/>									
<i>zDIP5</i> CycHex	495	733	503	863	305	51.6	3.4	0.15	0.14
Toluene	497	739	506	861	350	48.4	2.8	0.17	0.18
THF	495	675	504	849	337	41.2	2.3	0.18	0.26
CHCl ₃	496	714	505	866	343	42.2	2.2	0.19	0.26
DCM	495	777	505	885	388	30.3	1.8	0.17	0.39
DMF	495	781	505	882	386	26.0	-(a)	-	-
ACN	492	713	501	885	367	17.3	-(a)	-	-
<hr/>									
<i>zDIP6</i> CycHex	491	757	503	1311	467	8.5	0.8	0.11	1.14
Toluene	493	739	504	1240	463	8.5	0.8	0.11	1.14
THF	490	723	503	1290	516	4.9	-(a)	-	-
CHCl ₃	491	755	503	1220	485	5.0	-(a)	-	-
DCM	490	869	502	1290	485	3.7	-(a)	-	-

^(a) detected at 520 nm, there is a faster component than instrument resolution (0.4 ns), ^(b) detected at 520 nm, there is a faster component than instrument resolution (22 ps), ^(c) detected at 645 nm.

Table S2. X-ray data collection details for *zDIP3*.

Axis	dx/mm	2 θ /°	ω /°	ϕ /°	χ /°	Width/°	Frames	Time/s	Wavelength/ \AA	Voltage/kV	Current/mA	Temperature/K
Omega	50.301	30.00	30.00	0.00	54.73	0.50	360	10.00	0.71073	50	30.0	100.00
Omega	50.301	30.00	30.00	72.00	54.73	0.50	360	10.00	0.71073	50	30.0	100.00
Omega	50.301	30.00	30.00	144.00	54.73	0.50	360	10.00	0.71073	50	30.0	100.00
Omega	50.301	30.00	30.00	216.00	54.73	0.50	360	10.00	0.71073	50	30.0	100.00
Omega	50.301	30.00	30.00	288.00	54.73	0.50	360	10.00	0.71073	50	30.0	100.00
Phi	50.301	30.00	0.00	0.00	54.73	0.50	720	10.00	0.71073	50	30.0	100.00

Table S3. Sample and crystal data for *zDIP3*.

Identification code	<i>zDIP3</i>	
Chemical formula	C ₄₄ H ₅₀ N ₄ Zn	
Formula weight	700.25	
Temperature	100(2) K	
Wavelength	0.71073 Å	
Crystal size	0.180 x 0.220 x 0.370 mm	
Crystal habit	clear light pink prism	
Crystal system	orthorhombic	
Space group	P b c a	
Unit cell dimensions	a = 15.2910(14) Å	$\alpha = 90^\circ$
b = 15.0222(14) Å	$\beta = 90^\circ$	$\beta = 101.4330(10)^\circ$
c = 32.525(3) Å	$\gamma = 90^\circ$	$\gamma = 90^\circ$
Volume	7471.1(12) Å ³	
Z	8	
Density (calculated)	1.245 g/cm ³	
Absorption coefficient	0.693 mm ⁻¹	
F(000)	2976	

Table S4. Data collection and structure refinement for *zDIP3*.

Diffractometer	Bruker APEX II CCD	
Radiation source	fine-focus tube, MoK α	
Theta range for data collection	1.25 to 26.37°	
Index ranges	-19 $\leq h \leq$ 19, -18 $\leq k \leq$ 18, -40 $\leq l \leq$ 40	
Reflections collected	135932	
Independent reflections	7645 [R(int) = 0.0703]	
Coverage of independent reflections	100.0%	
Absorption correction	multi-scan	
Max. and min. transmission	0.8842 and 0.7854	
Structure solution technique	direct methods	
Structure solution program	SHELXS-97 (Sheldrick, 2008)	
Refinement method	Full-matrix least-squares on F ²	
Refinement program	SHELXL-97 (Sheldrick, 2008)	
Function minimized	$\Sigma w(F_o^2 - F_c^2)^2$	
Data / restraints / parameters	7645 / 0 / 456	
Goodness-of-fit on F²	1.065	
Δ/σ_{\max}	0.001	
Final R indices	6085 data; I>2 σ (I)	R1 = 0.0368, wR2 = 0.0851
	all data	R1 = 0.0546, wR2 = 0.0950
Weighting scheme	$w=1/[\sigma^2(F_o^2)+(0.0360P)^2+7.7287P]$	
	where $P=(F_o^2+2F_c^2)/3$	
Largest diff. peak and hole	0.362 and -0.419 eÅ ⁻³	
R.M.S. deviation from mean	0.056 eÅ ⁻³	

Table S5. X-ray data collection details for *zDIP4*.

Axis	dx/mm	2 θ /°	ω /°	ϕ /°	χ /°	Width/°	Frames	Time/s	Wavelength/Å	Voltage/kV	Current/mA	Temperature/K
Omega	50.412	30.00	30.00	0.00	54.73	0.50	360	10.00	0.71073	50	30.0	99.99
Omega	50.412	30.00	30.00	72.00	54.73	0.50	360	10.00	0.71073	50	30.0	100.01
Omega	50.412	30.00	30.00	144.00	54.73	0.50	360	10.00	0.71073	50	30.0	100.01
Omega	50.412	30.00	30.00	216.00	54.73	0.50	360	10.00	0.71073	50	30.0	100.01
Omega	50.412	30.00	30.00	288.00	54.73	0.50	360	10.00	0.71073	50	30.0	100.01
Phi	50.412	30.00	0.00	0.00	54.73	0.50	720	10.00	0.71073	50	30.0	100.01

Table S6. Sample and crystal data for *zDIP4*.

Identification code	<i>zDIP4</i>		
Chemical formula	$\text{C}_{52}\text{H}_{66}\text{N}_4\text{Zn}$		
Formula weight	812.46		
Temperature	100(2) K		
Wavelength	0.71073 Å		
Crystal size	0.19 x 0.28 x 0.31 mm		
Crystal habit	clear orange Prism		
Crystal system	monoclinic		
Space group	P 1 21/n 1		
Unit cell dimensions	$a = 14.1571(8) \text{ Å}$	$\alpha = 90^\circ$	
	$b = 12.7265(7) \text{ Å}$	$\beta = 90.3010(10)^\circ$	
	$c = 25.3289(14) \text{ Å}$	$\gamma = 90^\circ$	
Volume	$4563.5(4) \text{ Å}^3$		
Z	4		
Density (calculated)	1.183 Mg/cm^3		
Absorption coefficient	0.577 mm^{-1}		
F(000)	1744		

Table S7. Data collection and structure refinement for *zDIP4*.

Diffractometer	Bruker APEX II CCD	
Radiation source	fine-focus tube, MoK α	
Theta range for data collection	1.61 to 30.57°	
Index ranges	-20 $\leq h \leq$ 20, -18 $\leq k \leq$ 18, -36 $\leq l \leq$ 35	
Reflections collected	107913	
Independent reflections	13814 [R(int) = 0.0458]	
Coverage of independent reflections	98.6%	
Absorption correction	multi-scan	
Max. and min. transmission	0.8988 and 0.8411	
Structure solution technique	direct methods	
Structure solution program	SHELXS-97 (Sheldrick, 2008)	
Refinement method	Full-matrix least-squares on F ²	
Refinement program	SHELXL-97 (Sheldrick, 2008)	
Function minimized	$\Sigma w(F_o^2 - F_c^2)^2$	
Data / restraints / parameters	13814 / 0 / 532	
Goodness-of-fit on F²	1.024	
Δ/σ_{\max}	0.002	
Final R indices	10455 data; I>2 σ (I)	R1 = 0.0408, wR2 = 0.1011
	all data	R1 = 0.0631, wR2 = 0.1122
Weighting scheme	$w=1/[\sigma^2(F_o^2)+(0.0542P)^2+2.1872P]$	
	where $P=(F_o^2+2F_c^2)/3$	
Largest diff. peak and hole	0.528 and -0.337 eÅ ⁻³	
R.M.S. deviation from mean	0.059 eÅ ⁻³	

Table S8. X-ray data collection details for *zDIP5*.

Axis	dx/mm	2 θ /°	ω /°	ϕ /°	χ /°	Width/°	Frames	Time/s	Wavelength/Å	Voltage/kV	Current/mA	Temperature/K
Omega	50.000	30.00	30.00	0.00	54.74	-0.50	360	30.00	0.71073	50	30.0	100.01
Omega	50.000	30.00	30.00	72.00	54.74	-0.50	360	30.00	0.71073	50	30.0	100.01
Omega	50.000	30.00	30.00	144.00	54.74	-0.50	360	30.00	0.71073	50	30.0	100.01
Omega	50.000	30.00	30.00	216.00	54.74	-0.50	360	30.00	0.71073	50	30.0	100.01
Omega	50.000	30.00	30.00	288.00	54.74	-0.50	360	30.00	0.71073	50	30.0	100.01
Omega	50.000	30.00	30.00	0.00	54.74	-0.50	360	30.00	0.71073	50	30.0	100.01

Table S9. Sample and crystal data for *zDIP5*.

Identification code	<i>zDIP5</i>		
Chemical formula	$\text{C}_{63}\text{H}_{82}\text{Cl}_2\text{N}_4\text{O}_4\text{Zn}_2$		
Formula weight	1160.97		
Temperature	100(2) K		
Wavelength	0.71073 Å		
Crystal size	0.290 x 0.300 x 0.390 mm		
Crystal system	triclinic		
Space group	P -1		
Unit cell dimensions	a = 13.958(3) Å	$\alpha = 66.687(2)^\circ$	
	b = 15.459(3) Å	$\beta = 74.418(2)^\circ$	
	c = 16.517(3) Å	$\gamma = 78.087(3)^\circ$	
Volume	3132.5(11) Å ³		
Z	2		
Density (calculated)	1.231 g/cm ³		
Absorption coefficient	0.898 mm ⁻¹		
F(000)	1228		

Table S10. Data collection and structure refinement for *zDIP5*.

Diffractometer	Bruker APEX II CCD
Radiation source	fine-focus tube, MoK α
Theta range for data collection	1.52 to 26.00°
Index ranges	-17 $\leq h \leq 17$, -19 $\leq k \leq 19$, -20 $\leq l \leq 20$
Reflections collected	41573
Independent reflections	12284 [R(int) = 0.0510]
Absorption correction	multi-scan
Max. and min. transmission	0.7821 and 0.7209
Structure solution technique	direct methods
Structure solution program	SHELXS-97 (Sheldrick, 2008)
Refinement method	Full-matrix least-squares on F ²
Refinement program	SHELXL-97 (Sheldrick, 2008)
Function minimized	$\Sigma w(F_o^2 - F_c^2)^2$
Data / restraints / parameters	12284 / 0 / 699
Goodness-of-fit on F²	1.133
Δ/σ_{\max}	0.249
Final R indices	<div> <div>9284 data; I>2σ(I)</div> <div>all data</div> <div> $\parallel R1 = 0.0665, wR2 = 0.1458$ $\parallel R1 = 0.0933, wR2 = 0.1717$ </div> </div>
Weighting scheme	$w=1/[\sigma^2(F_o^2)+(0.0425P)^2+13.5881P]$ where $P=(F_o^2+2F_c^2)/3$
Extinction coefficient	0.0007(3)
Largest diff. peak and hole	1.294 and -1.037 eÅ ⁻³
R.M.S. deviation from mean	0.107 eÅ ⁻³

Table S11. X-ray data collection details for *zDIP6*.

Axis	dx/mm	2 θ /°	ω /°	ϕ /°	χ /°	Width/°	Frames	Time/s	Wavelength/Å	Voltage/kV	Current/mA	Temperature/K
Omega	50.423	30.00	30.00	0.00	54.73	0.50	360	2.00	0.71073	50	30.0	99.99
Omega	50.423	30.00	30.00	72.00	54.73	0.50	360	2.00	0.71073	50	30.0	99.99
Omega	50.423	30.00	30.00	144.00	54.73	0.50	360	2.00	0.71073	50	30.0	99.99
Omega	50.423	30.00	30.00	216.00	54.73	0.50	360	2.00	0.71073	50	30.0	99.99
Omega	50.423	30.00	30.00	288.00	54.73	0.50	360	2.00	0.71073	50	30.0	99.99
Phi	50.423	30.00	0.00	0.00	54.73	0.50	720	2.00	0.71073	50	30.0	99.99

Table S12. Sample and crystal data for *zDIP6*.

Identification code	<i>zDIP6</i>		
Chemical formula	$\text{C}_{33}\text{H}_{44}\text{N}_2\text{O}_2\text{Zn}$		
Formula weight	566.07		
Temperature	100(2) K		
Wavelength	0.71073 Å		
Crystal size	0.170 x 0.270 x 0.350 mm		
Crystal habit	clear orange Prism		
Crystal system	monoclinic		
Space group	C 1 2/c 1		
Unit cell dimensions	$a = 13.8580(5) \text{ Å}$	$\alpha = 90^\circ$ $\beta = 116.7540(10)^\circ$ $\gamma = 90^\circ$	
	$b = 17.1278(6) \text{ Å}$		
	$c = 14.5810(7) \text{ Å}$		
Volume	$3090.4(2) \text{ Å}^3$		
Z	4		
Density (calculated)	1.217 Mg/cm^3		
Absorption coefficient	0.825 mm^{-1}		
F(000)	1208		

Table S13. Data collection and structure refinement for *zDIP6*.

Diffractometer	Bruker APEX II CCD
Radiation source	fine-focus tube, MoK α
Theta range for data collection	2.03 to 31.35°
Index ranges	-19 ≤ h ≤ 20, -24 ≤ k ≤ 24, -21 ≤ l ≤ 21
Reflections collected	38024
Independent reflections	4848 [R(int) = 0.0443]
Coverage of independent reflections	95.5%
Absorption correction	multi-scan
Max. and min. transmission	0.8712 and 0.7601
Structure solution technique	direct methods
Structure solution program	SHELXS-97 (Sheldrick, 2008)
Refinement method	Full-matrix least-squares on F ²
Refinement program	SHELXL-97 (Sheldrick, 2008)
Function minimized	$\Sigma w(F_o^2 - F_c^2)^2$
Data / restraints / parameters	4848 / 0 / 182
Goodness-of-fit on F²	1.050
Δ/σ_{\max}	0.001
Final R indices	4099 data; I > 2σ(I) R1 = 0.0318, wR2 = 0.0753 all data R1 = 0.0437, wR2 = 0.0801
Weighting scheme	w = 1/[σ ² (F _o ²) + (0.0379P) ² + 2.2351P] where P = (F _o ² + 2F _c ²)/3
Largest diff. peak and hole	0.430 and -0.348 eÅ ⁻³
R.M.S. deviation from mean	0.063 eÅ ⁻³

Table S14: Fitting parameters for the PL lifetime measurements of *zDIP1-3* in different solutions

	Solvents	a₁	τ₁(ns)	a₂	τ₂(ps)*
<i>zDIP1</i>	Cyclohexane	1	3.7 ± 0.2		
	Dichloromethane	0.227	2.2 ± 0.1	0.773	≤ 22
	Acetonitrile	0.013	1.7 ± 0.05	0.987	≤22
<i>zDIP2</i>	Cyclohexane	1	4.8 ± 0.3		
	Dichloromethane	0.181	2.5 ± 0.2	0.819	≤ 22
	Acetonitrile	0.089	1.4 ± 0.02	0.910	≤ 22
<i>zDIP3</i>	Cyclohexane	1	1.4 ± 0.2		
	Dichloromethane	0.150	2.4 ± 0.1	0.850	≤ 22
	Acetonitrile	0.067	1.4 ± 0.05	0.933	≤22

* The faster component was faster than our instrument response function (FWHM ~22 ps)

References.

1. *Observation of Triplet Exciton Formation in a Platinum Sensitized Organic Photovoltaic Device*, S. T. Roberts, C. W. Schlenker, V. Barlier, R. E. McAnally, Y. Y. Zhang, J. N. Mastron, M. E. Thompson and S. E. Bradforth, *J. Phys. Chem. Lett.*, **2011**, 2, 48-54.